

# **Oak Street Bridge Half Bent Test On As Built and Retrofitted Specimens**

by

**Udhaya S. Arambawela.**

B.Eng. (Civil), University of Birmingham, Birmingham, England 1991

A THESIS SUBMITTED IN PARTIAL FULFILLMENT OF  
THE REQUIREMENTS FOR THE DEGREE OF  
MASTER OF APPLIED SCIENCE

in

THE FACULTY OF GRADUATE STUDIES  
DEPARTMENT OF CIVIL ENGINEERING

We accept this thesis as conforming  
to the required standard

THE UNIVERSITY OF BRITISH COLUMBIA

June 1994

© Udhaya Arambawela, 1994

In presenting this thesis in partial fulfilment of the requirements for an advanced degree at the University of British Columbia, I agree that the Library shall make it freely available for reference and study. I further agree that permission for extensive copying of this thesis for scholarly purposes may be granted by the head of my department or by his or her representatives. It is understood that copying or publication of this thesis for financial gain shall not be allowed without my written permission.

Department of CIVIL ENGINEERING.

The University of British Columbia  
Vancouver, Canada

Date 25 APRIL 94.

## ABSTRACT

As part of a research program on the seismic behaviour and retrofit of existing bridges, this investigation was designed to focus on column-cap beam joint regions. During the initial planning stages, a related investigation was sponsored by the Ministry of Transportation and Highways of BC to perform slow cyclic loading on large scale models of the Oak St. Bridge two-column bents. Therefore it was decided that this investigation would focus on the column-cap beam joints of the Oak St. Bridge, so that the results would have applicability to the actual bridge, and at the same time comparisons would be available between the joint tests of this investigation, and the full bent tests of the Ministry investigation. The joint tests described in this investigation comprise tests of half the two column bent, or "half bent test".

This investigation consists of the design of a test frame suitable for the half bent tests and other in plane load tests on structural assemblies such as concrete joints and their connecting members, a slow cyclic test on a 0.45 scale model of half of one of the Oak St. Bridge bents as originally constructed, and a slow cyclic test on a similar model retrofitted by post-tensioning. The latter duplicates one of the retrofit schemes also tested in the Ministry sponsored program on a 0.45 scale model of the full bent.

The test frame proved suitable for the test program and for similar future testing. With a variety of options available for application of in-plane loading and restraints, it is capable of testing large scale specimens of realistic sizes for bridges and buildings. In the tests described in this thesis, it demonstrated the potential ability to duplicate the essential behaviour of the more expensive full bent tests.

**TABLE OF CONTENTS**

<b>Abstract</b>	<b>ii</b>
<b>List of Tables</b>	<b>vi</b>
<b>List of Figures</b>	<b>vii</b>
<b>Acknowledgement</b>	<b>xi</b>
<b>1 Introduction</b>	<b>1</b>
1.1 Background	1
1.2 Objectives and the Scope of Investigation	2
1.3 Test Facility	3
1.4 Choice of Prototype Structure	5
1.5 Seismic deficiencies of the Oak street bents	12
1.6 Concept of Joint Performance	13
1.7 Joint Mechanism	15
<b>2 Analysis and Design of the Test Frame</b>	<b>17</b>
2.1 Introduction	17
2.2 Capacities of the Frame	19
<b>3 Test Specimen</b>	<b>25</b>
3.1 Introduction	25
3.2 Properties of the Prototype Bent	25
3.3 Properties of the UBC Full Bent Model	26
3.4 Properties of the Half Bent Model	26
3.5 Construction of the Specimen	32
3.5.1 Formwork	32
3.5.2 Reinforcing Steel	34

3.5.3 Concrete	36
<b>4 Instrumentation and Data Acquisition Systems</b>	<b>41</b>
4.1 Introduction	41
4.2 Instrument Locations	45
4.2.1 Strain Gauge Locations	45
4.2.2 LVDT Locations	49
<b>5 Testing Procedure</b>	<b>52</b>
5.1 Boundary Conditions	52
5.2 Loading Sequences	58
5.3 Loading on the Full Bent Model	58
5.4 Loading on the the Specimen OJ1	59
5.5 Loading on the Specimen OJ2	66
<b>6 Experimental Obserations</b>	<b>73</b>
6.1 Specimen OJ1	73
6.1.1 Observed Behaviour	73
6.1.2 Sectional Analysis	78
6.1.3 Strain Gauge Readings	80
6.2 Specimen OJ2	82
6.2.1 Observed Behaviour	82
6.2.2 Sectional Analysis	85
6.2.3 Strain Gauge Readings	88
6.3 Comparison with Bent Test Results	90
<b>7 Summary and Conclusions</b>	<b>96</b>
<b>References</b>	<b>100</b>
<b>Appendix A: Analysis and Design of The Test Frame</b>	<b>104</b>
<b>Appendix B: Force Resultants of OJ and OSB Specimens</b>	<b>107</b>



## LIST OF TABLES

Table	Page
Table 3.1 Concrete properties of OJ1 .....	36
Table 3.2 Concrete properties of OJ2 .....	37
Table 4.1 Strain gauge channel numbering .....	46
Table 4.2 Strain gauge locations.....	47
Table 5.1 Jack J1 loading for specimen OJ1 .....	62
Table 5.2 J1 Loading for specimen OJ2 .....	69
Table 6.1 OJ1 Maximum demand for pulling.....	78
Table 6.2 Maximum demand for pushing .....	78
Table 6.3 Input loading OJ1 joint 7.....	79
Table 6.4 Out put capacities OJ1 joint 7 .....	79
Table 6.5 Maximum demand for pulling.....	86
Table 6.6 Maximum demand for pushing .....	86
Table 6.7 Input loading OJ2 joints 7 and 11 .....	87
Table 6.8 Output capacities OJ2 joints 7 and 11.....	87
Table A.1 Maximum frame member forces.....	106
Table C.1 Jack J2 min/max load.....	115
Table C.2 Jack J2 and J3 min/max load.....	115

## LIST OF FIGURES

Figure	Page
Fig. 1.1 Photograph of the Oak St. Bridge.....	6
Fig. 1.2 General arrangement.....	7
Fig. 1.3 Bent S28-reinforcing details of prototype (Elevation).....	9
Fig. 1.4 Bent S28 reinforcing details of prototype (Plan).....	10
Fig. 1.5 Bent S28 reinforcing details prototype (Sections).....	11
Fig. 1.6 Compression strut mechanism.....	16
Fig. 1.7 Truss mechanism .....	16
Fig. 2.1 Basic specimen configurations .....	18
Fig. 2.2 Final magnitudes and ranges of jack loads (inside of frame).....	20
Fig. 2.3 Construction drawing (Elevation) .....	21
Fig 2.4 Construction drawing (Plans).....	22
Fig. 2.5 Construction drawing (Connections).....	23
Fig. 2.6 Photo of the steel frame.....	24
Fig. 3.1 Specimen OJ1.....	27
Fig. 3.2 Specimen OJ2.....	28
Fig. 3.3 MOTH model elevation .....	29
Fig. 3.4 MOTH model plan.....	30
Fig. 3.5 MOTH model sections.....	31
Fig. 3.6 A photograph of the form work .....	33
Fig. 3.7 A photograph of the steel cages .....	35
Fig. 3.8 Photograph showing pouring of the concrete .....	38
Fig. 3.9 Post-tensioning of bars.....	39
Fig. 3.10 Installing the specimen in the frame.....	40

Fig. 3.11 Specimen and the frame .....	40
Fig. 4.1 Photograph of a strain gauge in a bar .....	43
Fig. 4.2 Photo of the data acquisition system .....	44
Fig. 4.3 Strain gauge locations (Elevation).....	48
Fig. 4.4 Strain gauge locations (Plan).....	49
Fig. 4.5 LVDT locations.....	50
Fig. 4.6 Photo of LVDT locations .....	51
Fig. 5.1 Specimen OJ1 bearing locations.....	53
Fig. 5.2 Specimen OJ2 bearing locations.....	54
Fig. 5.3 Bearing arrangement.....	55
Fig. 5.4 Photograph of the pin bearing .....	56
Fig. 5.5 Horizontal and vertical jack connection.....	57
Fig. 5.6 Dead and lateral loads on full bent test .....	59
Fig. 5.7 Loading OJ1 .....	60
Fig. 5.8 Applied jack loads specimen OJ1 .....	63
Fig. 5.9 Shear/Moment variation of OJ1 cap beam .....	64
Fig. 5.10 Cap beam shear of specimen OJ1 and OSB1 .....	64
Fig. 5.11 Loading OJ2 .....	67
Fig. 5.12 Applied jack loads specimen OJ2 .....	70
Fig. 5.13 Shear /Moment variation at x-x of OJ2.....	71
Fig. 5.14 Cap beam shear of specimen OJ2 and OSB2 .....	71
Fig. 5.15 Column shear of specimen OJ2 and OSB2 .....	72
Fig. 6.1 OJ1 Load displacement at the column tip .....	75
Fig. 6.2 Photograph of crack patterns at sequence F .....	75
Fig. 6.3 Photograph of crack patterns at sequence O.....	76

Fig. 6.4 Photograph of crack patterns at sequence P .....	76
Fig. 6.5 Load displacement at the column tip (Column Test).....	77
Fig. 6.6 Photograph of crack patterns at Push Over .....	77
Fig. 6.7 Strain gauge BB3 .....	81
Fig. 6.8 OJ2 Load displacement at the column tip .....	83
Fig. 6.9 Photograph of crack patterns at sequence D.....	83
Fig. 6.10 Photograph of crack patterns at sequence L .....	84
Fig. 6.11 Photograph of crack patterns at Push Over .....	84
Fig. 6.12 Photograph of crack patterns at Push over .....	85
Fig. 6.13 Strain gauge CO4 .....	88
Fig 6.14 Strain gauge CI3.....	89
Fig 6.15 Hysteresis loop of bent test 2 (OSB2) .....	90
Fig.6.16 Cap beam cracking specimen OJ1 .....	92
Fig. 6.17 Cap beam cracking Specimen OSB1 .....	92
Fig. 6.18 Crack pattern of OJ1 and OSB1.....	93
Fig. 6.19 Column cracking specimen OJ2 .....	94
Fig. 6.20 Column cracking specimen OSB2 .....	95
Fig. B.1 Maximum loading on OJ1 .....	107
Fig. B.2 Maximum loading on OSB1.....	107
Fig. B.3 Axial force on OJ1.....	108
Fig. B.4 Axial force on OSB1.....	108
Fig. B.5 Shear force on OJ1.....	109
Fig. B.6 Shear force on OSB1.....	109
Fig. B.7 Bending moment on OJ1.....	110
Fig. B.8 Bending moment on OSB1.....	110

Fig. B.9 Maximum loading on OJ2..... 111

Fig. B 10 Maximum loading on OSB2.....111

Fig. B 11 Axial force on OJ2.....112

Fig. B 12 Axial force on OSB2.....112

Fig. B.13 Shear force on OJ2.....113

Fig. B.14 Shear force on OSB2.....113

Fig. B 15 Bending moment on OJ2.....114

Fig. B.16 Bending moment on OSB2.....114

## ACKNOWLEDGEMENT

The author is very grateful to his supervisor, Professor R. G. Sexsmith for his guidance, suggestions and encouragement extended throughout his research. The financial support provided by the Natural Sciences and Engineering Research Council of Canada, Ministry of Transportation and Highways of British Columbia, and the University of British Columbia is also gratefully acknowledged. The author also wishes to express his gratitude to Professors P.E. Adebar and D.L. Anderson for reviewing the manuscript.

Appreciation is extended to Mr. Dick Postgate, Mr. Paul Symons, Mr. Markus Seethaler and Ms. Dongchang Gao for their helpful participation and assistance during the experimental investigation.

The author also wishes to thank his parents for their moral and financial support throughout his University career, and the friends for sharing laughs and making life easier.

# **CHAPTER 1**

## **INTRODUCTION**

### **1.1 Background**

Southern coastal British Columbia is situated over the Cascadia Subduction zone. Earthquakes that may present a hazard to this area may occur in three distinct source regions: deep earthquakes within the subducted plate, earthquakes within the continental crust, and subduction earthquakes on the boundary layer between the two lithospheric plates (Rogers, 1993).

The recent history of the area includes a number of earthquakes up to Richter magnitudes about 7, but these have occurred relatively far from urban areas and have not been the cause of widespread damage. The rapid growth of population and corresponding development has increased the potential for serious damage.

The response and the magnitude of damage to a structure due to an earthquake depends on a number of parameters:

1. Magnitude and location of the earthquake
2. Duration of strong shaking
3. The geology and soil conditions of the site
4. The level of earthquake resistant construction

Of the above four, only the soil and the construction, in particular the strength and ductility of the structure, can be improved.

As a result of the 1971 San Fernando, 1987 Whittier Narrows and 1989 Loma Prieta earthquakes, the importance of upgrading the bridge structures was demonstrated. In the case of two column bridge bents, shear failure of the beam, column or beam-column joint are possible failure modes which may have to be rectified to achieve acceptable performance of the complete structure.

Most of the major bridges in southern coastal British Columbia were built prior to 1970, when the knowledge of seismic design was very low. Preliminary assessment and screening of British Columbia's bridges indicates that a great many require seismic upgrades (MOTH, 1992). Because these structures were designed and constructed under a variety of now obsolete criteria, they pose many problems in the analysis of their behaviour and design of retrofits.

## **1.2 OBJECTIVES AND THE SCOPE OF INVESTIGATION**

This project has been developed to assist in the prediction of behaviour of original and retrofitted structures, particularly near the joint regions of reinforced concrete bridge support bents such as the two column bents that support many bridge superstructures.

The project includes the development of a test facility to test a variety of configurations of L and T joints of large scale, followed by tests on a portion of a typical two column bent from the Oak Street Bridge. The two column bent tests were sponsored

by the Ministry of Transportation and Highways of BC (MOTH), and are reported elsewhere (Seethaler, 1994 and Anderson et al., 1994). The tests of this investigation were conducted on one "as-built" specimen and on one "retrofit" specimen, using half of the actual bent scaled to 0.45 of the original full size. The cap beam of the second specimen was retrofitted using 6 Dywidag bars of diameter 5/8". Each Dywidag bar was post-tensioned to 35 kips which is 80% of the ultimate strength of the bar. These bars were supported at the end of the cap beam using 1.5" thick steel plates. The choice of specimen was made to conform to corresponding tests on a 0.45 scale full bent from the same bridge, so that comparisons could be made between the half bent and full bent tests, in addition to predictions of prototype performance.

Testing consists of slow cyclic testing to simulate the reverse cyclic loading of an earthquake transverse to the longitudinal direction of the bridge. The loading rate, amplitude, and the number of cycles per sequence were kept as close as possible to the full bent test loading pattern so that the comparison of results are meaningful.

### **1.3 Test Facility**

The purpose of the test facility is to provide a means to apply jack loads from various directions to a planar concrete structure, so that joint configurations of several types could be loaded in their plane. The design objectives were developed to achieve a facility that would have maximum value for future investigations, within a limited budget (about \$30,000).

Overall design considerations were as follows:

1. The busy structures testing laboratory has limited room for new facilities, therefore it is desirable to have a facility that is self equilibrating, i.e. does not depend on the floor reactions to develop the applied load. This led to the decision to develop a rectangular frame that surrounds the specimen. Jack loads between specimen and frame do not impose external reactions. This permits the frame to be located anywhere in the laboratory.

2. In order to permit maximum future flexibility as to specimen size, and to permit possible retrofits that may widen the specimen, a vertical, rather than horizontal, configuration was chosen. This permits full and equal access to both sides of frame and specimen, and avoids limits on the specimen width.

3. The maximum height of the frame above the floor of the laboratory is limited by the overhead crane. In addition, the placement of specimens into the frame requires the overhead crane.

4. The height limit, and the desire to construct a frame as strong as possible within the budget, led to the choice of overall frame dimensions. Some preliminary analyses of concrete sections of the contemplated size led to load requirements for the frame. The test facility design criteria and description are discussed in Chapter 2.

## 1.4 Choice of Prototype Structure

During the time the test frame was under development a number of actual bridges were considered as possible prototypes. As the time came to make a decision on a prototype, the British Columbia Ministry of Transportation and Highways (MOTH) decided to sponsor testing of Oak Street Bridge bents as part of a bridge retrofit program for that structure. The MOTH program plan includes testing of a 0.45 scale model of bent S28 of the Oak Street Bridge (Anderson et al., 1994). The existence of the Oak Street full bent tests then led to the decision to test half bents, i.e. half cap beam and one column from the Oak St. bent, as part of this project. This achieves the ability to have a basis of comparison not only with analysis of the prototype, but with full bent tests.

The Oak street bridge was designed in 1954. It is 1.84 km long and supported on 83 reinforced concrete piers. The bridge is 62'6" wide, and accommodates 4 traffic lanes and 2 sidewalks. It consist of steel spans in the center and concrete spans in the North and South approaches.

The approach spans consist of a series of four span continuous haunched concrete girders, supported on five concrete bents each with two columns. In the south approach, the 6.5" thick deck slab is supported on 5 reinforced concrete beams. These beams are supported on concrete bents having varying heights. The superstructure is continuous over five supports with expansion joints located at the end of the each four span section. Figures 1.1 and 1.2 show the elevation of the bridge and the general arrangement.

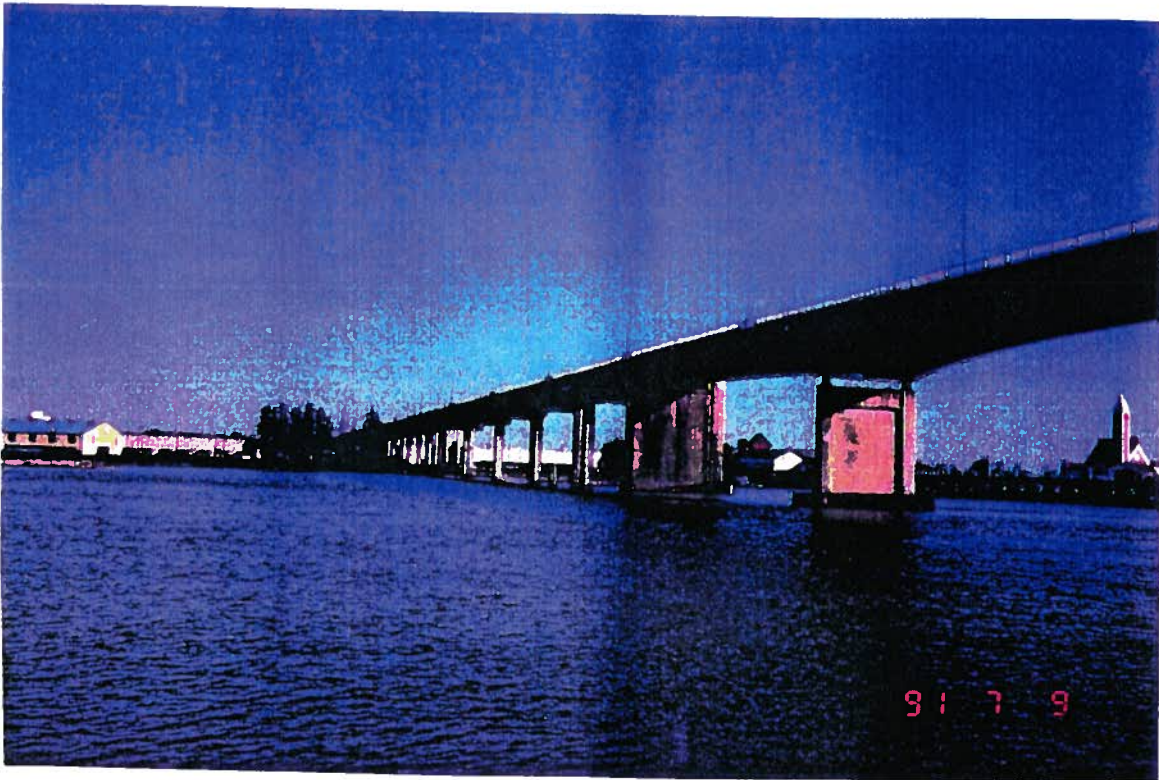


Figure 1.1 Photograph of the Oak St. Bridge

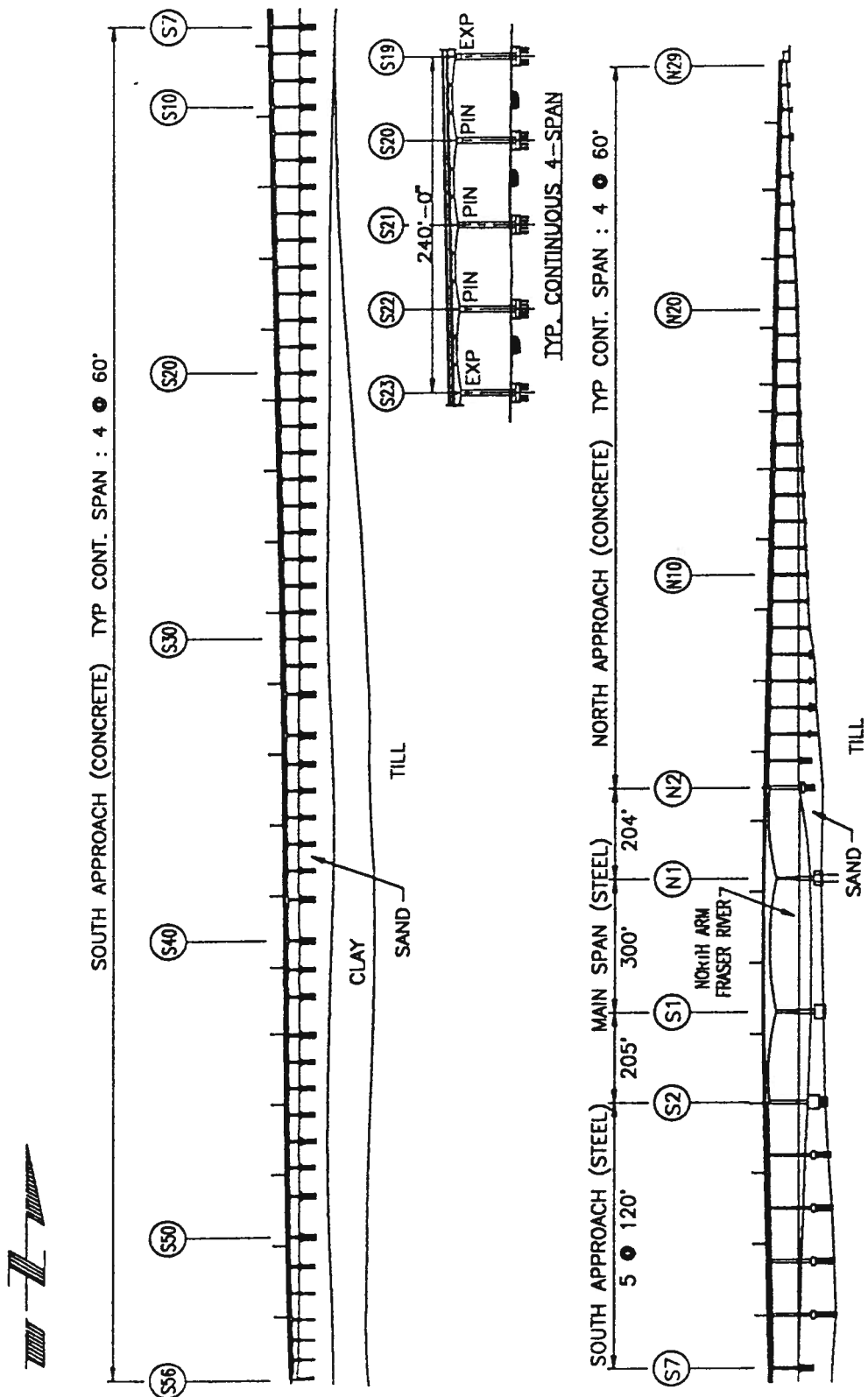


Figure 1.2 General arrangement

The bent S28 was chosen for the MOTH project and for this half bent project, as this is a typical bent with an average height. The heights of the bents varies from about 20' to 60'. This is a first interior support of a continuous four span deck, therefore this support will attract the highest dead load.

The cap beam of bent S28 has a cross section of 3'6"x5' with two 8'6" long tapering cantilevers at the ends. Two 4'x4' reinforced concrete rectangular columns of length 32.2' provide support for the superstructure at bent S28. See Figs. 1.3 to 1.5, Bent S28 reinforcing details. The columns are supported on 14'6"x14'6"x3' foundations which are on 24 timber piles driven into sandy clay which is overlain on glacial till (Kennedy et al., 1992).

In this thesis, the designation OSB1, OSB2 etc is given to Oak St. Bridge full bent tests done by others. OJ1, OJ2 refers to the half bent tests performed as part of this investigation.

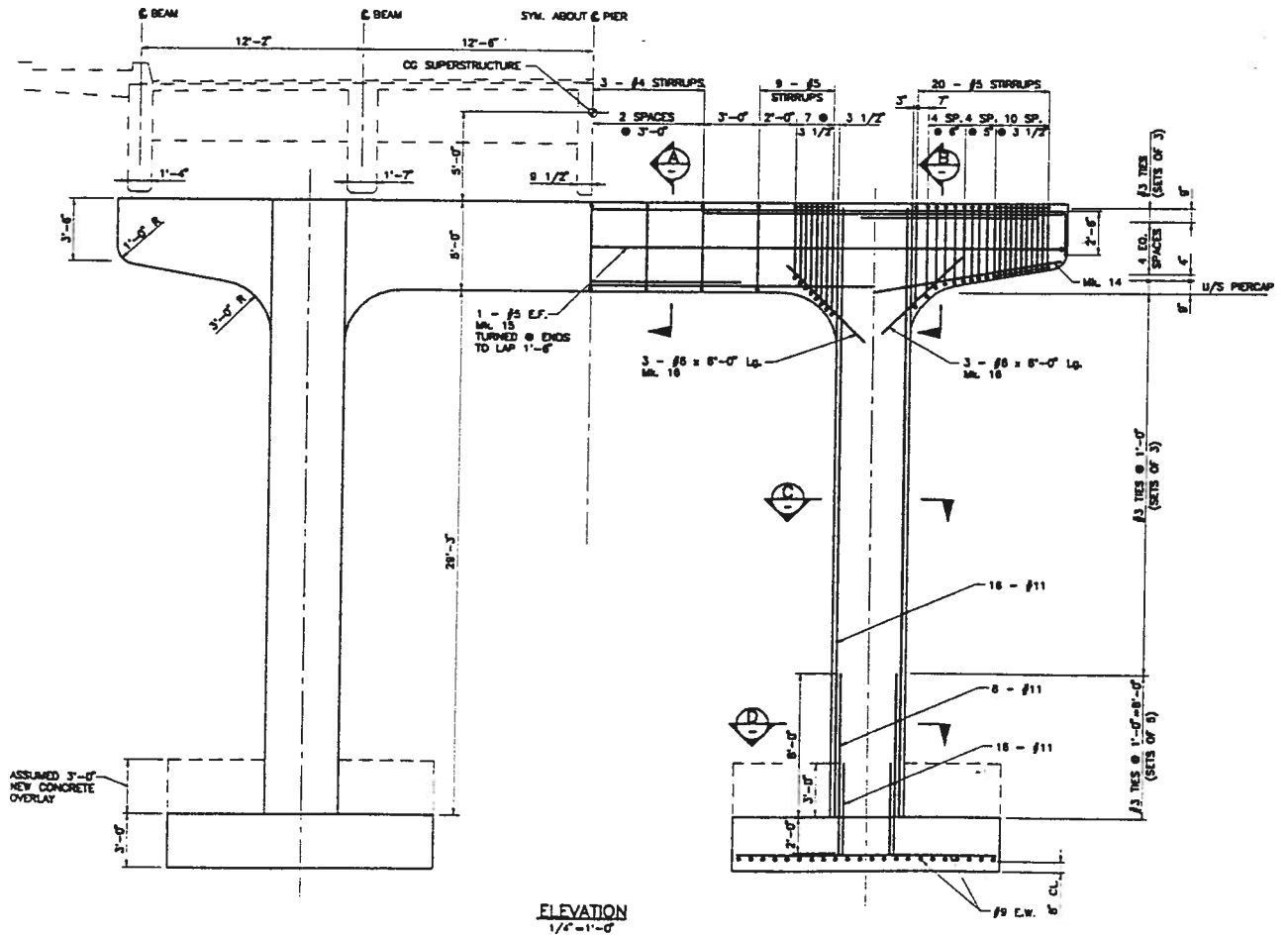
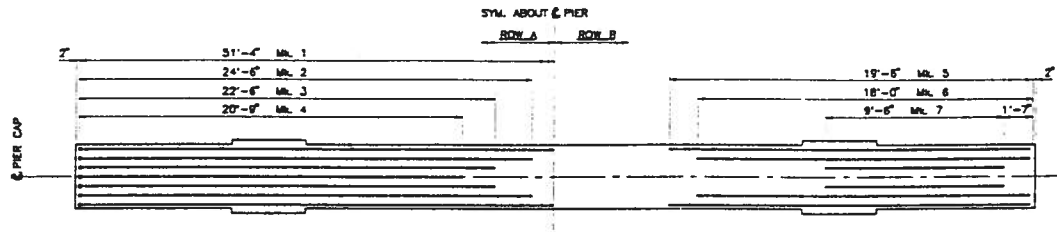
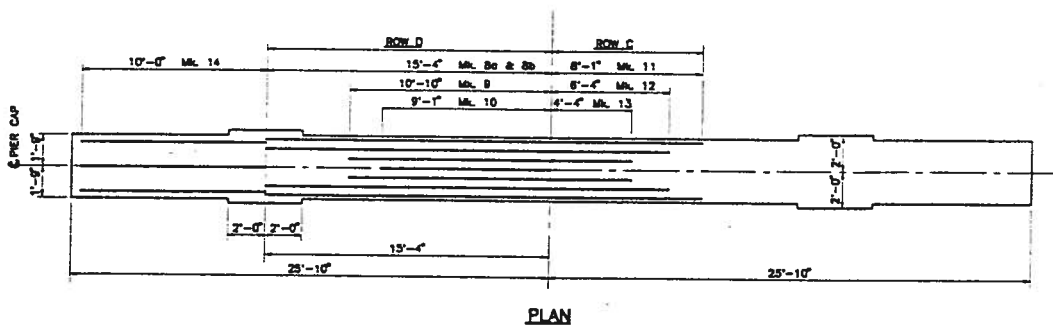


Figure 1.3 Bent S28-reinforcing details of prototype (Elevation)



Cap beam showing top steel



Cap beam showing bottom steel

Fig. 1.4 Bent S28 reinforcing details of prototype (Plan)

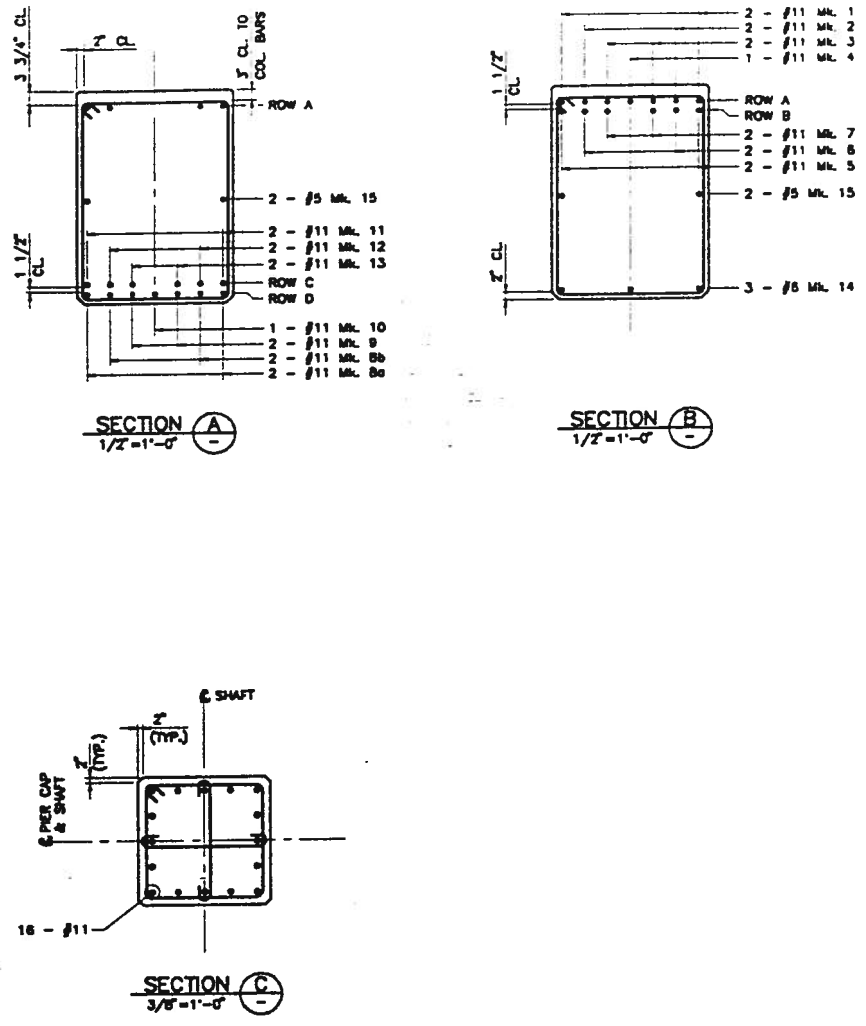


Fig. 1.5 Bent S28 reinforcing details prototype (Sections)

## **1.5 SEISMIC DEFICIENCIES OF THE OAK STREET BRIDGE BENTS**

Apart from loss of span failures, most of the seismic problems in this type of concrete bridge occur in the bridge bents. Poor detailing of reinforcement contributed to severe damage of piers and joints of concrete bridge structures during the Loma Prieta earthquake (Mitchell et al., 1994). Specific deficiencies and retrofit schemes for Oak St. Bridge are discussed elsewhere (Kennedy et al., 1992). Some of the deficiencies in the bent which can be identified from the Oak street bridge drawings are:

1. The shear capacity of the columns may be inadequate. These contain about 1% (Figure 1.5 ) longitudinal reinforcement but have only #3 ties at a spacing of 12" which is inadequate for these large columns. This insufficient shear reinforcement will result in the possibility of a brittle shear failure in the column and it will not allow energy absorption through flexural hinging which is the preferred method of seismic energy dissipation. Buckling of longitudinal bars and spalling of concrete is also common due to widely spaced tie reinforcement.

2. The cap beam also contains about 1% longitudinal steel at Sections A and B. (Figure 1.5) The shear reinforcement in Section A consists of #4 closed stirrups at a spacing of 3 feet. Due to inadequate shear capacity in the cap beam, brittle shear failure might occur in the cap beam due to lateral seismic loading.

3. Anchorage of the cap beam longitudinal bottom bars in the joint region does not appear to be sufficient.

4. Poor shear capacity in the joint region. The column tie reinforcement (# 3 bars @ 1') has been continued but no extra ties are provided to carry the large shear force.

5. The positive moment capacity of the cap beam at the face of the column is not sufficient (Kennedy et al., 1992)

As the shear capacity of the cap beam was found to be critically deficient, the as built half bent specimen, OJ1, was tested for cap beam shear. The second specimen, OJ2, was retrofitted to improve the shear capacity of the cap beam, and then tested for cap beam shear, column shear and column flexure.

## 1.6 CONCEPT OF JOINT PERFORMANCE

Reinforced concrete joint behaviour depends on the interaction of properties such as shear, bond and confinement. To understand the interaction of these properties it is important to first understand them acting independently, and this is still of interest to several investigators. In addition to the complex interaction of shear, bond, and confinement, nonlinearities in concrete and the large variety in geometry and load distributions makes it extremely difficult to understand joint behaviour.

Reinforced concrete frames typically have joints in which the connecting members should have sustained strength under deformation reversals into the inelastic range. The connecting members dissipate energy through reversal of deformation into the inelastic range. In bridges, the development of plastic hinges in the columns is the preferred method of energy dissipation.

Different modes of failure possible in or near the joint region are:

1. Beam hinging
2. Column hinging
3. Column crushing
4. Reinforcement anchorage failure
5. Joint shear failure

The failure of a joint and its connecting members will preferably absorb energy through beam or column inelastic rotation. Failure of reinforcement bar anchorage or the joint region in shear will reduce the energy absorbing capacity and the load carrying capacity of the system. Spalling of concrete in the joint region will reduce the compressive load carrying capacity.

The first experimental tests on beam column connections were done by the Portland Cement Association around forty years ago and were published subsequently by Hanson and Conner (Hanson and Conner, 1967). Those results indicated that properly designed and detailed joints can resist moderate earthquakes without loss of strength. The amount and arrangement of the transverse steel in the joint and the method of anchoring beam bars were tested by Park and Paulay (Park and Paulay, 1973). Their results indicated that a beam stub protruding beyond the far face of the column can be used to effectively anchor the beam bars. Large variations in the axial load and the amount of transverse reinforcement within the joint had little effect on the ultimate shear strength of the joint (Jirsa et al., 1975). Subsequent investigations were carried out to find the factors influencing the shear capacity of the beam column connections. The shear strength of the connection is primarily governed by the cross sectional area of the joint (Meinheit and

Jirsa, 1981). The main objectives of most of the above experiments were to improve the ductility of the joint under reverse cyclic loading and to provide better anchorage for the beam reinforcement in exterior connections.

### **1.6.1 JOINT MECHANISM**

Due to seismic forces there will be moment reversals across the joint and therefore the joint region is subjected to horizontal and vertical shear forces which are much larger than the forces in adjacent beams and columns. Due to the above moments there will be a force gradient in the reinforcement with high bond stresses. If bond failure does occur there will be excessive drift in the joint region, along with strength deterioration.

During seismic loading the force transfer from the beam to the column through the joint can be modeled by truss action, consisting of concrete struts and tension ties formed by the transverse reinforcement steel within the joint, which is activated by the bond stress and anchorage (Priestley and Paulay, 1991). This truss mechanism (Fig. 1.7) is relatively soft, compared with the alternative direct compression strut (Fig. 1.6). The direct compression strut does not require reinforcement within the joint and therefore it does not rely on the bond characteristics. The strut, however, does have to be anchored at the joint boundaries. This is a stiff mechanism and when concrete damages load will transfer through the joint by the softer truss mechanism. In practice, the behaviour of the joint probably falls somewhere between these two mechanisms.

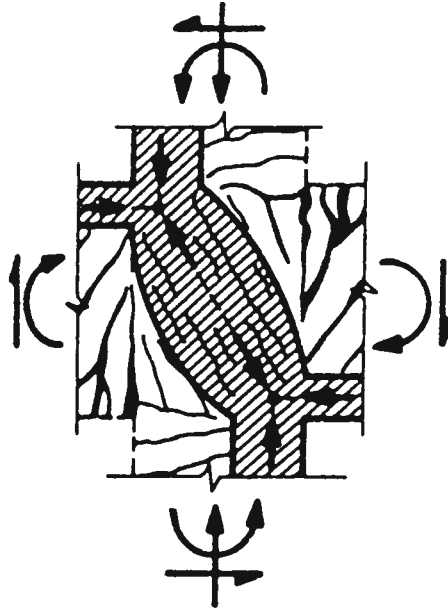


Fig. 1.6 Compression strut mechanism

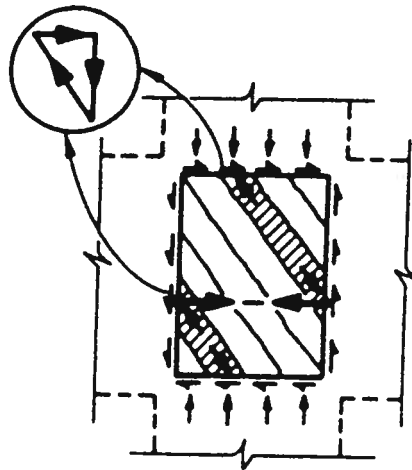


Fig. 1.7 Truss mechanism

## **CHAPTER 2**

### **TEST FRAME**

#### **2.1 INTRODUCTION**

Present small scale-modeling techniques cannot adequately represent the complex force transfer along the joint region of concrete structures or the deterioration of this force transfer as the load on the joint is cycled. Therefore to examine the behaviour of large scale concrete components (i.e. joints and regions close to the joint) of bridges under slow reverse cyclic loading, a self equilibrating steel frame was designed and constructed.

The testing can be performed either vertically or horizontally. Although a horizontal test setup might be easier to construct, a vertical frame is preferred as there is more clearance between the specimen and the floor (for retrofit work etc.) and a better view of the specimen while testing. As the steel frame designed is self equilibrated it can be used as a horizontal frame if required.

Two basic specimen configurations can be tested using this test setup. Those are,

**Interior beam column connection - T joint**

**Exterior beam column connection- L joint**

The specimens can be tested either up side down or right way up depending on the requirements. The specimen configuration and the loading arrangement can be chosen to

model the loading and deformation in a real structure in side sway due to lateral earthquake loading. The vertical and horizontal jacks at the top will provide pinned connections at the tip of the column. The testing is confined to two dimensions as the interaction of the beams and columns are along the same frame.

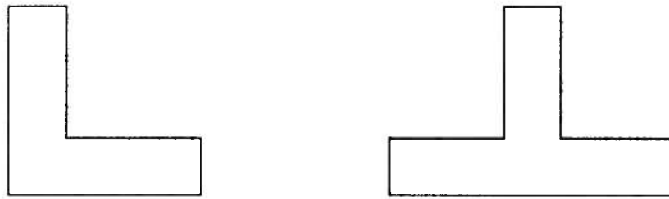


Fig. 2.1 Basic specimen configurations

Within the specimen configurations shown above a wide range of specimen sizes can be tested using this test setup. An elevation is shown in Fig. 2.3. The number, type (i.e. pin or roller) and the places of the boundary conditions at the bottom of the specimen can be changed so that the required loading can be obtained in the beam stub. The vertical and the lateral position of the load application on the column can be changed as described in Section 2.2. As two vertical jacks can be used at the column tip it is possible to obtain a required moment and the axial load at the column tip and therefore it is not necessary to have an inflection point at this location. The lateral jack can be used to apply the shear in the column. It is also possible to apply a vertical load directly on the beam stub if necessary (i.e. dead load on the beam stub).

## 2.2 CAPACITIES OF THE FRAME

The design of the test setup had to be compatible with the existing laboratory facilities. Therefore the frame analysis provided for use of jacks similar to those used for the beam element testing facility, which are of 1000 kN capacity. The steel frame was designed to accommodate 2 vertical and 1 horizontal jacks of this capacity. Depending on the requirements these jacks can act either in tension or compression.

The force applied by the vertical jack on the column of the specimen reacts against the top girder of the test frame, while the force applied by the lateral jack on the column reacts against either of the columns of the steel frame. These jacks can be repositioned at 9-5/8" increments along the length of the girder and the column. The maximum values of jack forces and the length on which those forces can be applied are shown in Fig. 2.2. Figs. 2.3 to 2.5 indicate sizes and details of steel frame, and Fig. 2.6 is a photograph of the frame mounted vertically in the UBC Structural Engineering Laboratory.

The top girder can be repositioned between the two columns in three consecutive positions at 2' increments along the height of the column. Large steel sections were used to construct the columns and the girder of the frame to provide adequate stiffness of the frame relative to the stiffness of the specimen. The bottom box girder is provided with 1" holes at 3" spacing so that the boundary conditions of the specimen can be changed as required.



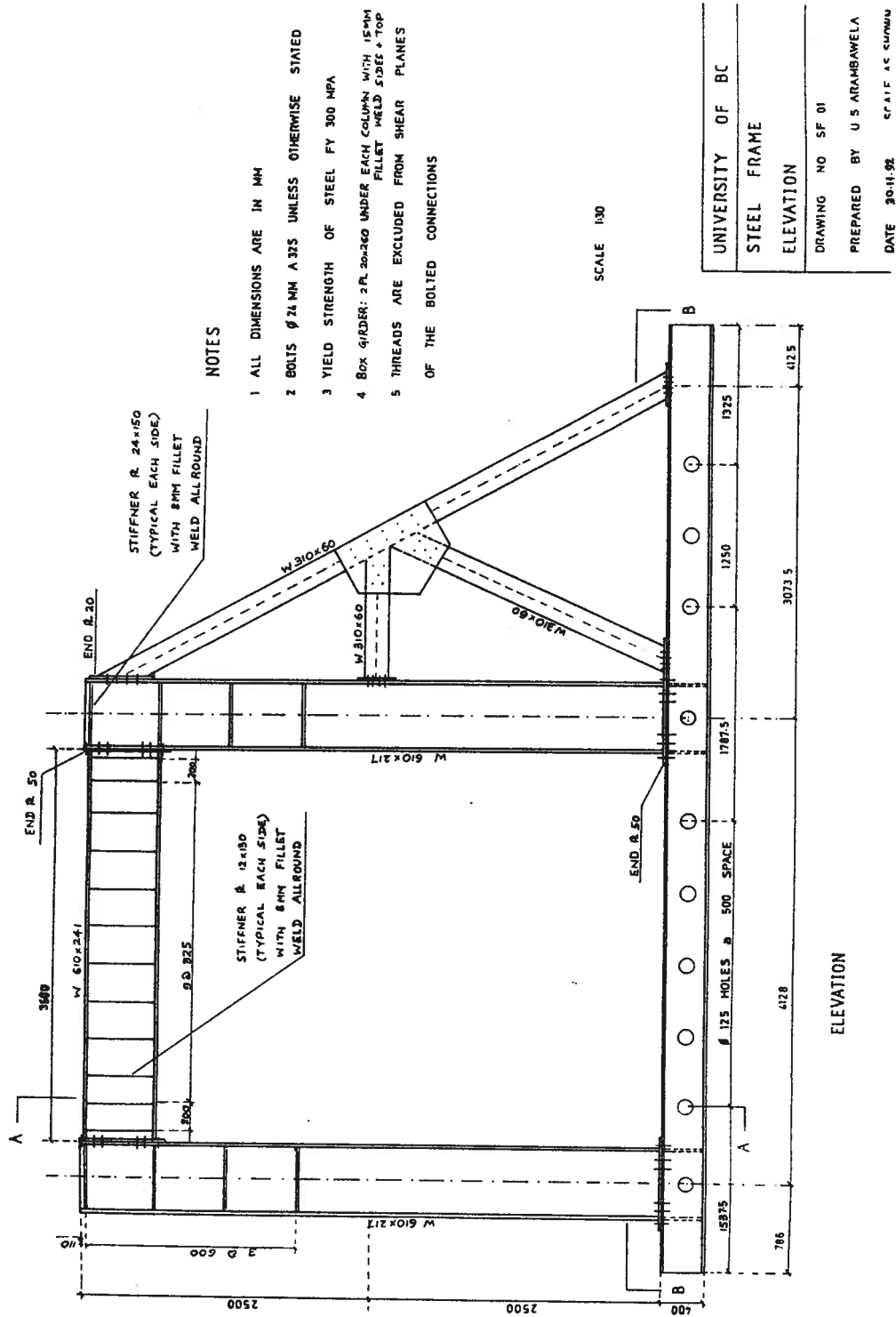


Figure 2.3 Construction drawing (Elevation)

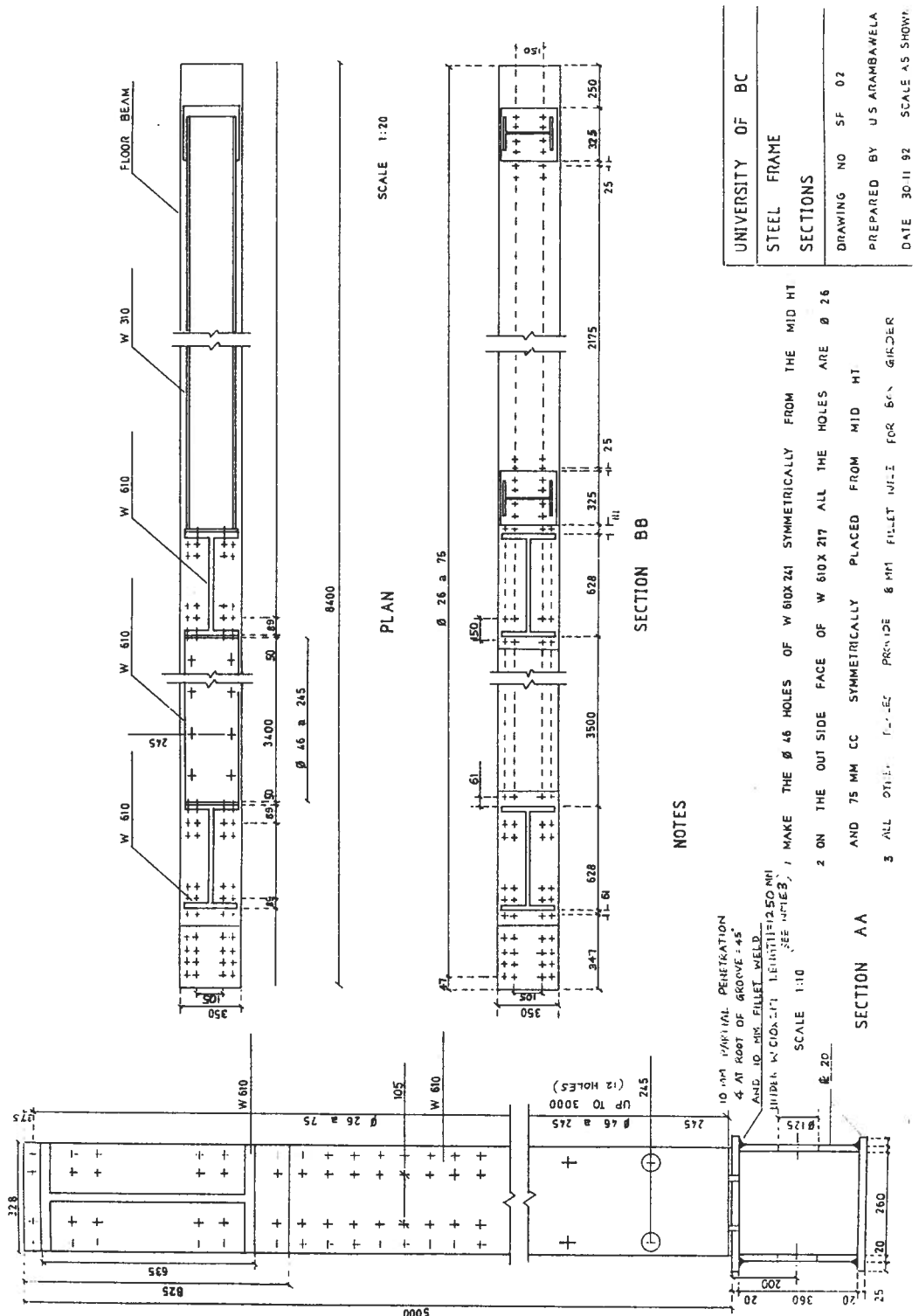


Fig 2.4 Construction drawing (Plans)

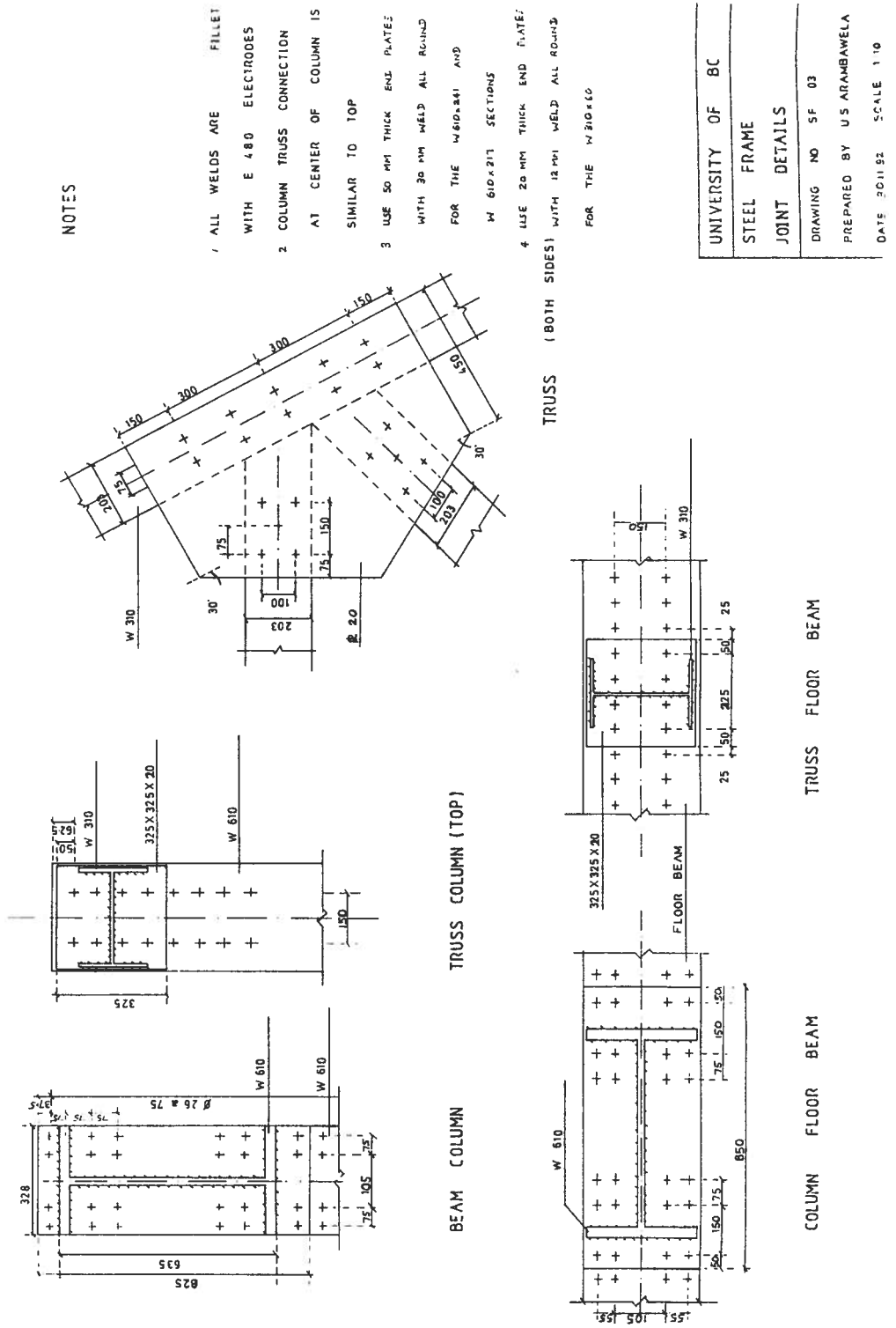


Fig 2.5 Construction drawing (Connections)

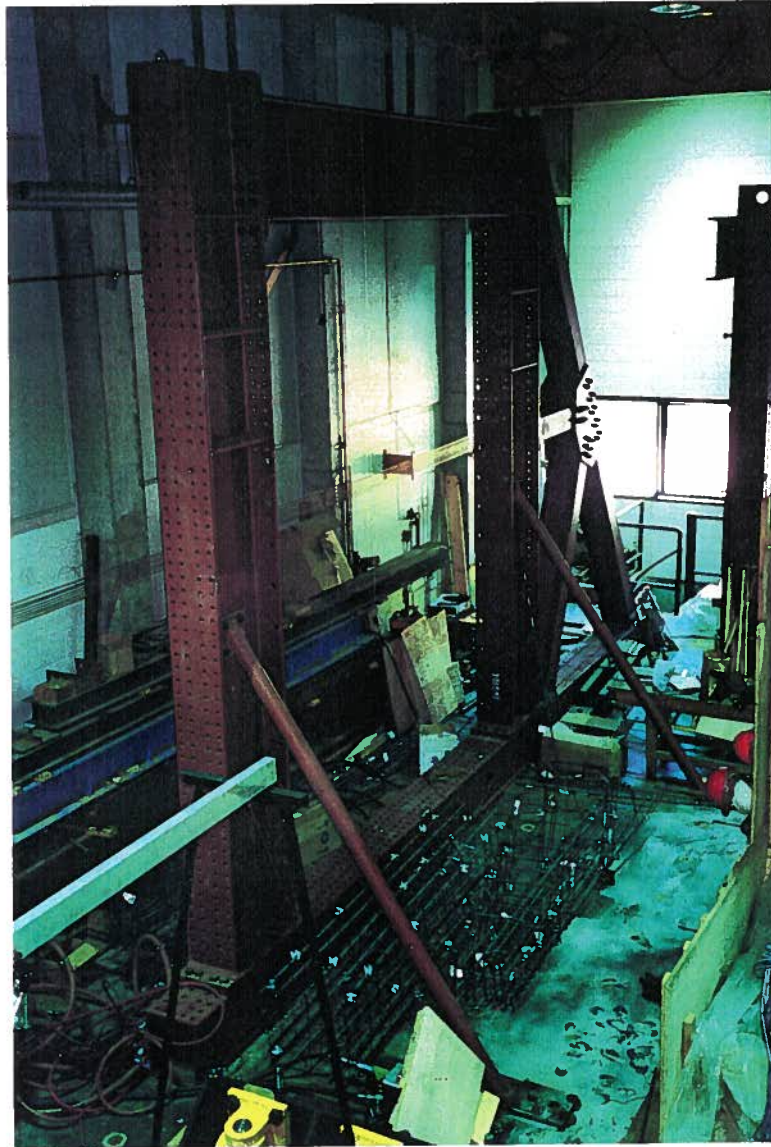


Fig 2.6 Photo of the steel frame

## **CHAPTER 3**

### **TEST SPECIMENS**

#### **3.1 INTRODUCTION**

As explained in the Chapter 1, bent S28 of the Oak St. Bridge at 0.45 scale was selected so that the comparison with the MOTH full bent test can be done without complications of scaling. The existing material properties were used for the construction of the specimens. The material properties are given in Section 3.5. Two half bent specimens were made to the above specifications and one of those was retrofitted by post-tensioning the cap beam.

#### **3.2 PROPERTIES OF THE PROTOTYPE BENT**

The cap beam of the prototype has a cross Section of 3'6" x 5' with 4 - #11 bars at the top and 13 - #11 bars at the bottom at section A. Figures 1.3 through 1.5 show prototype section details. In this region (Section A) there are #4 closed stirrups spaced at 3'. The cross section of the supporting column is 4' x 4' . The column contains 16 - #11 bars and #3 ties spaced at 1' . The originally specified material strengths from the drawings were compressive strength of concrete  $f'c = 20.7$  MPa and the yield strength of steel  $f_y = 276$  MPa. The material strengths indicated by the destructive test carried out by Klohn

Crippen International were much higher. Concrete had a compressive strength of 41.4 MPa and the column bars tested in S46 and N27 had yield strengths of 338 MPa and 400 MPa respectively.

### **3.3 PROPERTIES OF THE MOTH FULL BENT MODEL**

The MOTH model was at 0.45 scale and the cap beam had a cross section of 1'7" x 2'3" with 4 - #5 bars at the top and 13 - #5 bars at the bottom. The gauge 4 stirrups were spaced at 1'4". The column had a cross section of 1'9.5" x 1'9.5" with 16 - #5 bars. Gauge 9 ties in the column were spaced at 5 3/8". Fig. 3.3 through 3.5 show the MOTH full bent. The material strengths obtained from the prototype testing were used for the experiment, as it is important to have correct material properties in order to identify the critical failure modes. Therefore  $f_c'=40$  MPa and  $f_y=345$  MPa were used for the MOTH full bent model. The concrete cylinder strengths obtained from the first two MOTH specimens indicated much higher average values of 47.6 and 51.1 MPa respectively.

### **3.4 PROPERTIES OF THE HALF BENT MODEL**

The half bent should have a 11' 8" long cap beam with a cross section of 2'3" x 1'7" and a 9' long column with a cross section of 1'9.5" x 1'9.5". Due to the geometrical limitations of the frame the maximum cap beam length that can be accommodated is 11'. Therefore the length of the cap beam was reduced by 8" from the side opposite to the cantilever. As described in the Introduction (Chapter 1) two specimens were built. Both

specimens have similar material properties, but the cap beam of the second specimen was retrofitted by post tensioning. Geometry of specimen 1 and 2 are shown in the Figs. 3.1 and 3.2. Bearing dimensions are given in Section 6.1. The reinforcing steel for both specimens was contributed by MOTH is therefore same as for the MOTH model. Concrete properties of the half bent test are given in Table 3.1 and 3.2.

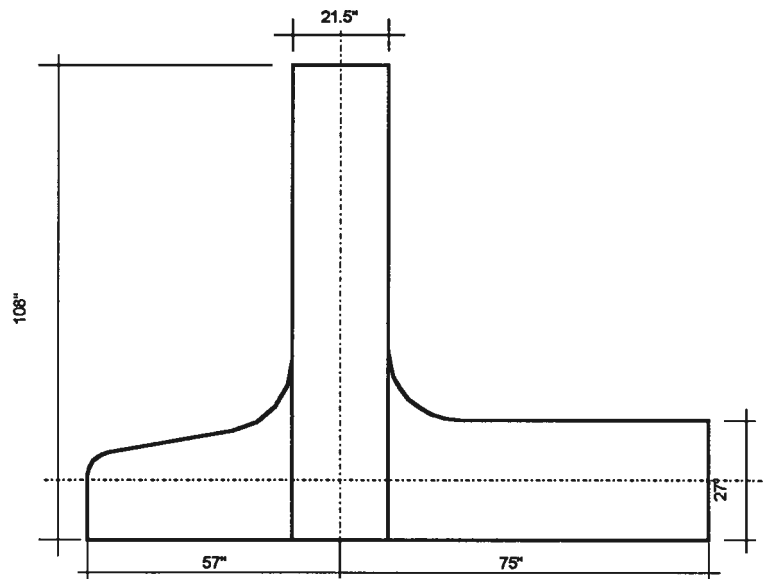


Fig. 3.1 Specimen OJ1

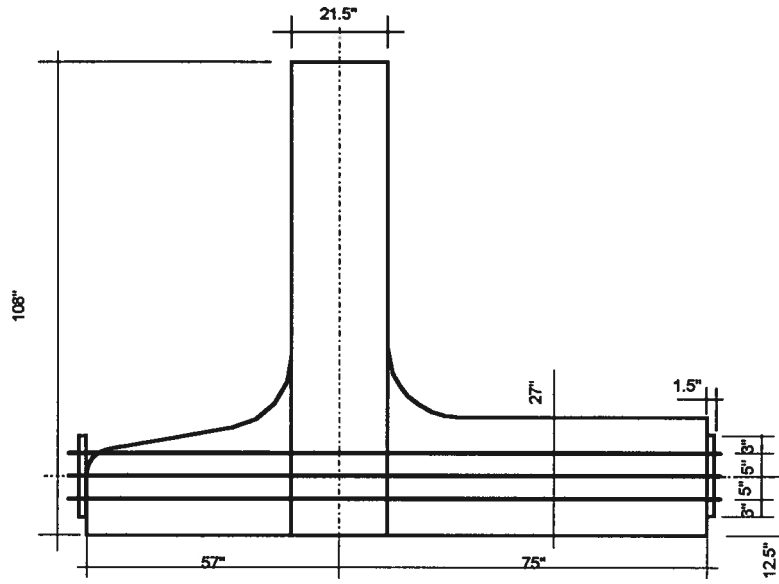


Fig. 3.2 Specimen OJ2

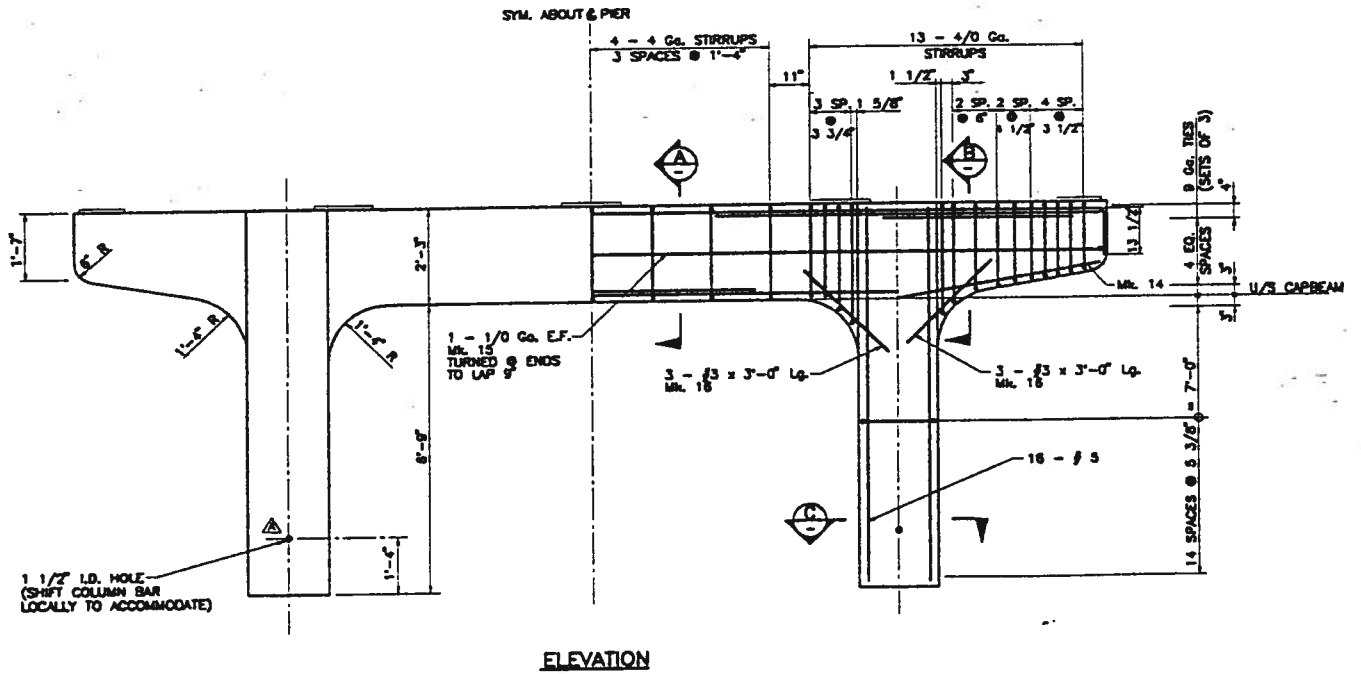
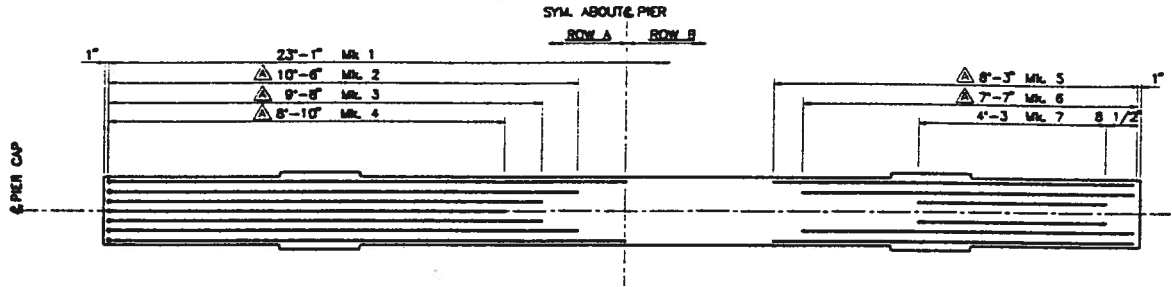
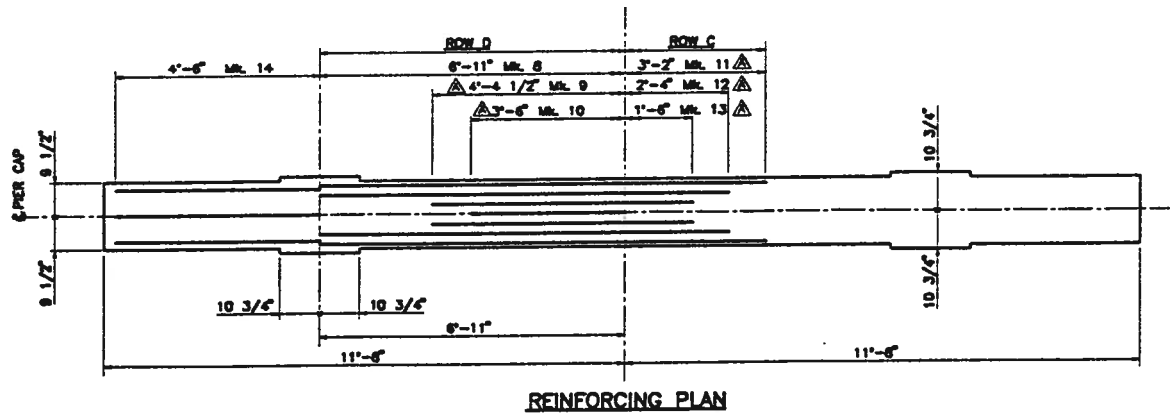


Fig. 4.3 MOth model elevation



Top steel



REINFORCING PLAN

Bottom steel

Fig. 3.4 MOTH model plan



## **3.5 CONSTRUCTION OF THE SPECIMEN**

### **3.5.1 FORM WORK**

As testing was planned to carry out upside down it was decided to construct the specimens upside down, i.e. beam laying flat on the floor. Half inch diameter tie rods which can carry 4500 pounds and quarter inch snap ties which can carry 2250 pounds in tension were used to support the liquid concrete pressure. One inch thick plywood was used so that the number of ties required for the lateral load supporting scheme could be minimized. Fig. 3.6 is a photograph of the form prior to placing concrete.



Fig. 3.6 A photograph of the form work

### 3.5.2. REINFORCING STEEL

The reinforcing cages for the beam and the column were assembled outside of the form work and all the strain gauges were installed before making the cages. First the two bearing plates were assembled in the form work, then the beam cage was placed, followed by the column cage. Figure 3.7 is a picture of the reinforcement in the form work. To obtain the concrete cover plastic chairs were attached to the reinforcement. The yield strength of the reinforcing main bars and stirrups were 345 MPa.

The cap beam of the second specimen was post-tensioned using 6 Dywidag bars of diameter 5/8". Each Dywidag bar was tensioned to 35 kips which is 0.8fpu. The resultant post tensioning force before relaxation of the bars is 210 kips acting 12.5" below the top face of the cap beam. This provides the same prestress as the MOTH full bent test.

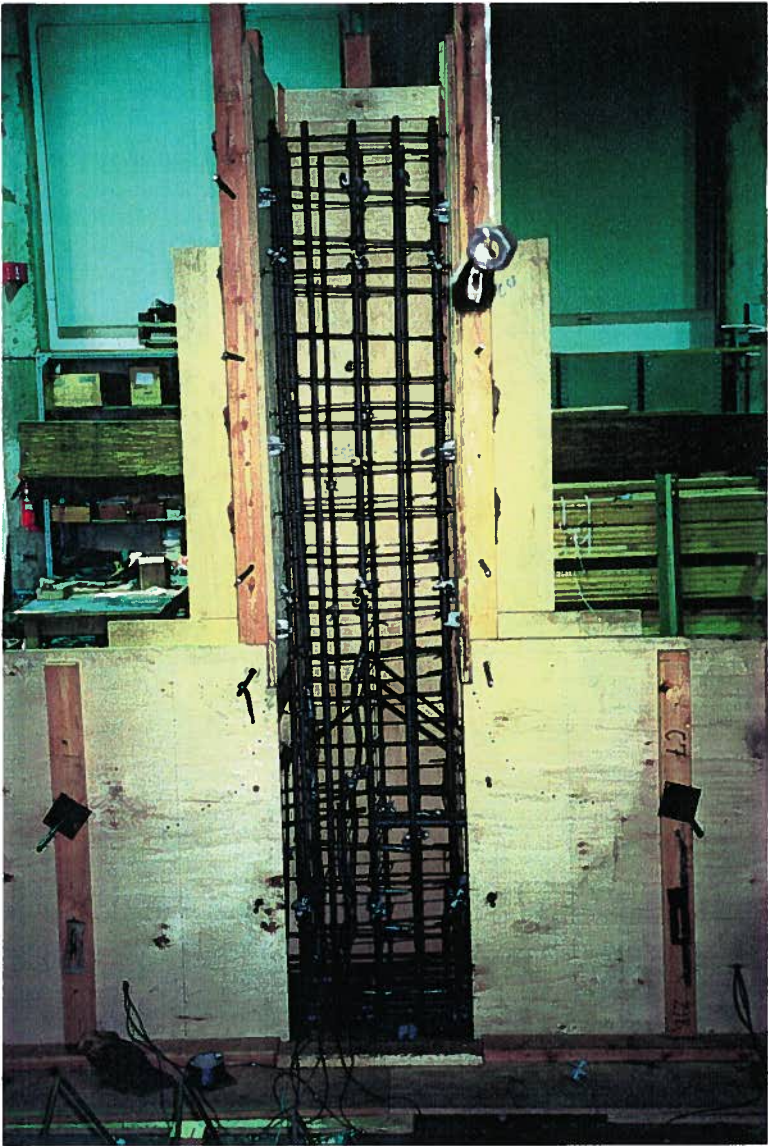


Fig 3.7 A photograph of the steel cages

### 3.5.3. CONCRETE

The ready mixed concrete was obtained from a local supplier. The concrete was ordered 5 MPa lower than the required strength because the suppliers tend to supply higher strength concrete. Unfortunately the strength of concrete received was much lower than the required strength. The height and the diameter of concrete cylinders tested were 12" and 6" respectively. A total of twelve cylinders were tested for the first specimen, out of which a set of six were air cured and six were moist cured. The two flat sides of all the cylinders were grinded before testing. Three cylinders of each set were tested under uniaxial compression after 28 days. The rest were tested after 2 months (while testing the specimen). The cylinders were not dried before testing.

Table 3.1 Concrete properties of OJ1

	Strength (MPa)	Slump (in)	Aggregate size (in)	Air Content(%)
Requested	35	5	0.5	0
Delivered		4.5	0.5	2.5
Average 28 day	26.0(D) 26.0(W)	—	—	—
Average at Testing(2 months)	31.5(D) 31.0(W)	—	—	—

Total of ten cylinders were tested for the second specimen. Out of which a set of four were air cured and six were moist cured. Two of air cured and three of moist cured cylinders were tested under uniaxial compression after 28 days. The rest were tested after 2 months (while testing the specimen). The cylinders were not dried before testing.

Table 3.2 Concrete properties of OJ2

	Strength (MPa)	Slump (in)	Aggregate Size(in)	Air Content(%)
Requested	35	5	0.5	0
Delivered	—	5	0.5	2
Average 28 day	32.8(D) 33.25(W)	—	—	—
Average at Testing (2 months)	30.4(D) 40.5(W)	—	—	—

D - Air cured

W - Moist cured

The cylinders were crushed using the Baldwin after 28 days and when testing of the specimen. The 28 day compressive strengths were much lower than the expected values. As a result of the difficulty of proper vibration of the upside down curve region of the specimen there were a couple of small honeycombs in that region. Fortunately most were in the cantilever side of the beam of both specimens except one small honeycomb on the

other side of the beam of specimen OJ2. The cantilever side of the beam is not of direct concern in these tests. Both specimens were white washed so that the crack patterns could be seen better.



Fig. 3.8 Photograph showing pouring of the concrete



Fig. 3.9 Post-tensioning of bars

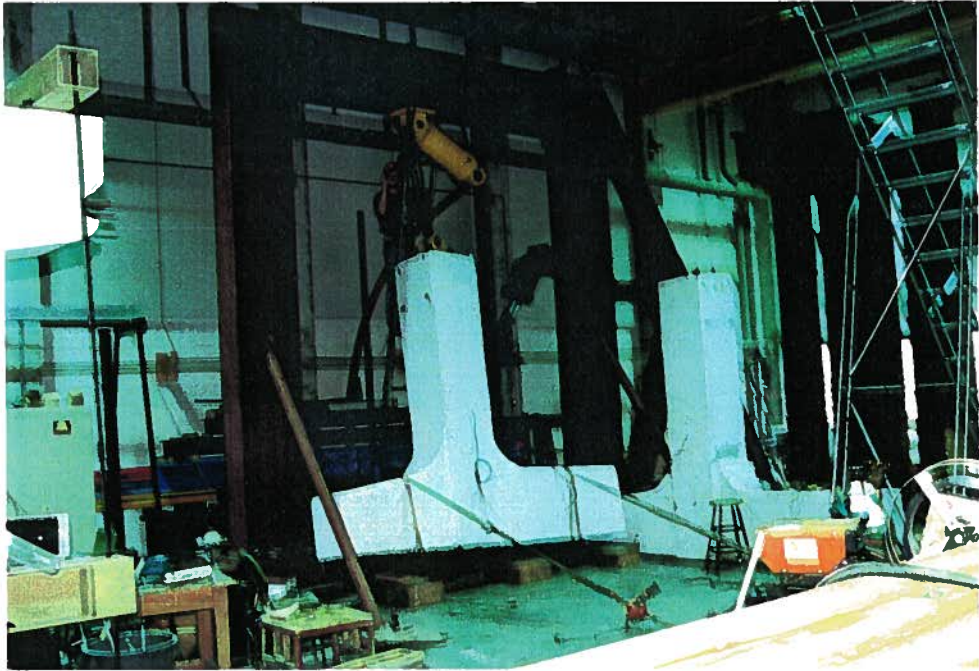


Fig. 3.10 Installing the specimen in the frame

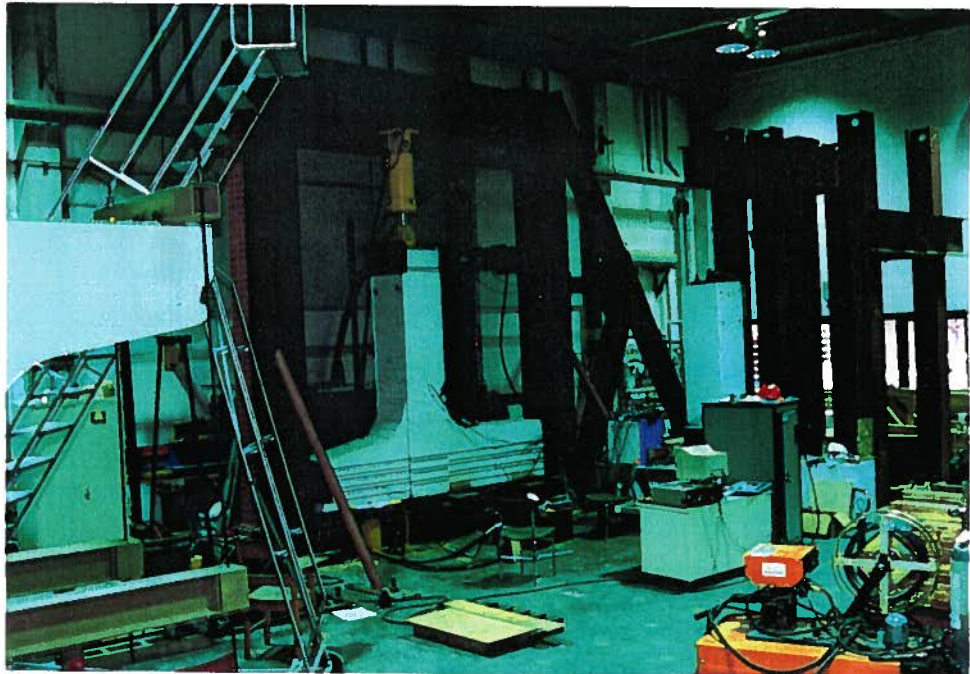


Fig. 3.11 Specimen and the frame

## **CHAPTER 4**

### **INSTRUMENTATION AND DATA ACQUISITION SYSTEMS**

#### **4.1 INTRODUCTION**

The equipment used to load the specimen and to store the data consisted of the following;

OPTILOG for data acquisition

MTS controller for the application of the loads

2 hydraulic actuators for the first specimen and 3 actuators for the second specimen

2 IBM Personal Computers

20 strain gauges per specimen

3 LVDT displacement transducers

1 Load cell

1 Pressure Transducer for the first specimen and 2 for the second specimen

The loading function for the lateral loading jack at the column tip was generated using a MTS 458.10C/0.20C Microconsole. The loading for the lateral jack was under displacement control. The hydraulic pressure of the other jacks was controlled manually in relation to the lateral loading jack so that the required loading function was achieved. The

jacks used for the application of the column reaction vertically (J2) and horizontally (J1) had a capacity of 200 kips and 100 kips respectively.

The measuring devices used were strain gauges, linear variable differential transformers (LVDT displacement transducers), and a load cell attached to the lateral loading MTS jack. The strain gauges type was FLA-5-11, the resistance and the gauge length were 120 ohm and 5 mm respectively. Fig 4.1 shows an individual strain gauge mounted on a reinforcing bar.



Fig. 4.1 Photograph of a strain gauge in a bar

For data acquisition the OPTILOG system was used with the OPUS 200 software. (Optim Users' Software) OPUS 200 is a BASIC computer program which controls the collection of voltages from several channels and converts them to loads, displacements and strains which are stored, printed and plotted.

26 different measurements were recorded using the OPTILOG 120 data acquisition system for the specimen OJ1. Those consist of 20 strain gauges, 4 LVDTs ,1 Load Cell and 1 pressure transducer. For the specimen OJ2 there was an additional pressure transducer for the third jack. The data acquisition system scanned the devices at a constant time interval of 2 seconds. Fig. 4.2 shows the data acquisition system.

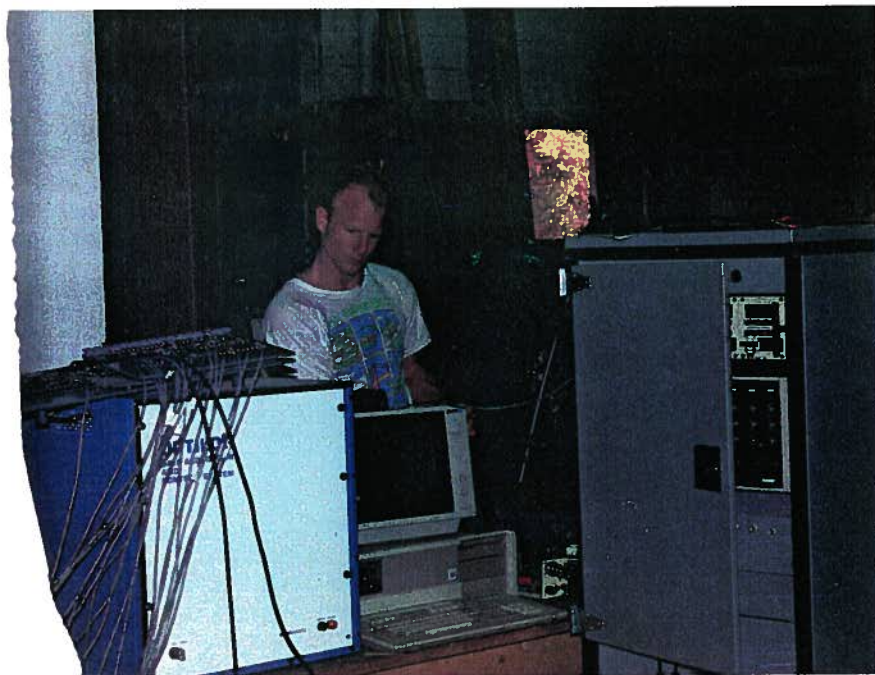


Fig. 4.2 Photo of the data acquisition system

## **4.2 INSTRUMENT LOCATIONS**

### **4.2.1 STRAIN GAUGE LOCATIONS**

Twenty strain gauges were attached to the beam and column main bars and ties in the joint region. See Fig.4.3 and 4.4. These strain gauge locations coincide with some of the strain gauge locations of the MOTH full bent test. This was done so that the bent and the joint test results can be compared with each other. Table 4.1 indicates the strain gauge designations and correspondence with the full bent test. Table 4.2 gives the strain gauge locations in the half bent specimen.

At the strain gauges locations the bars were machined and smoothed to provide a flat surface for mounting. The smoothed surface was then cleaned, the strain gauge and the terminal strips mounted with glue. Wires were then soldered. After applying the protection coating the strain gauges were covered with putty and aluminum paper for protection. The strain gauges were then checked to ensure that the connections were working before assembling the reinforcing cages. The cables leading from the gauges were taken along the bars so that damage to these while pouring the concrete would be minimum.

Table 4.1 Strain gauge channel numbering

Strain Gauge	Full Bent Test	Half Bent Test
CI1	21	K
CI3	23	J
CI4	24	G
CO1	26	N
CO3	28	L
CO4	29	I
CT2	32	H
CT3	33	O
CT4	34	M
BS1	50	A
BS2	51	C
BS3	52	B
BT1	1	P
BT3	3	Q
BT4	4	T
BT5	5	R
BT6	6	S
BB1	10	E
BB2	11	F
BB3	12	D

Table 4.2 Strain gauge locations (X-Y Coordinates with the center line of the column top as the origin.)

Strain Gauge	X (inches)	Y (inches)
CI1	8	7
CI3	8	31
CI4	8	37
CO1	-8	7
CO3	-8	31
CO4	-8	37
CT2	0	14
CT3	0	23
CT4	0	29
BS1	12	16
BS2	19	16
BS3	34	16
BT1	-13	2
BT3	0	2
BT4	6	2
BT5	14	2
BT6	22	2
BB1	6	24
BB2	14	24
BB3	21	24

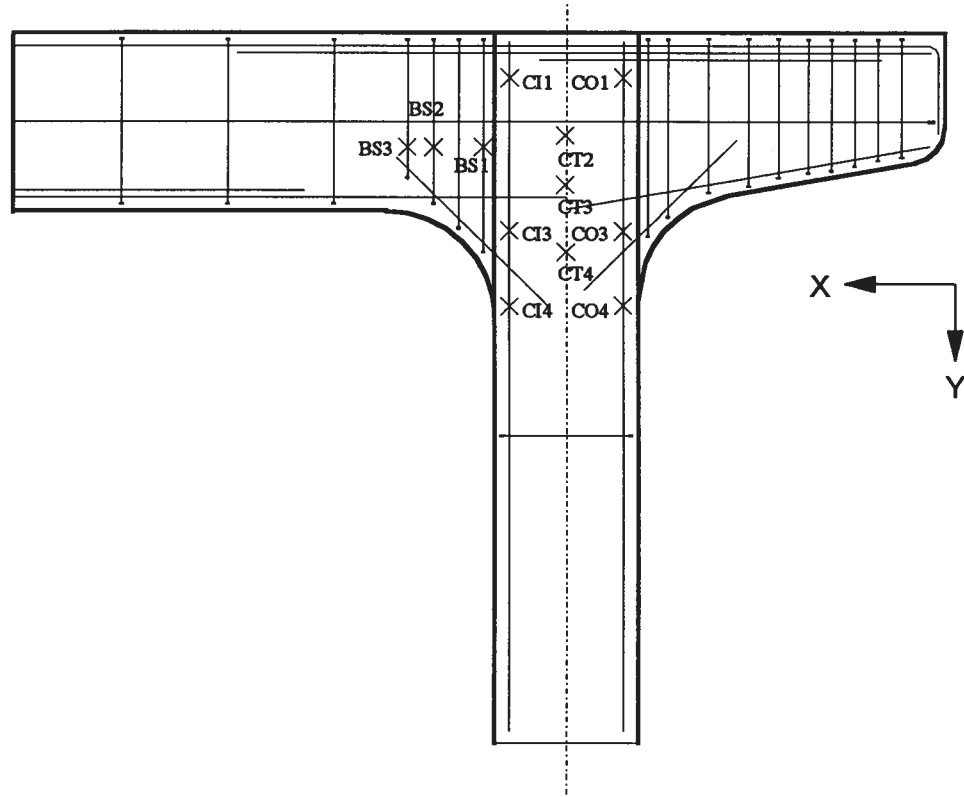


Fig. 4.3 Strain gauge locations (Elevation). Plan in Fig. 4.4

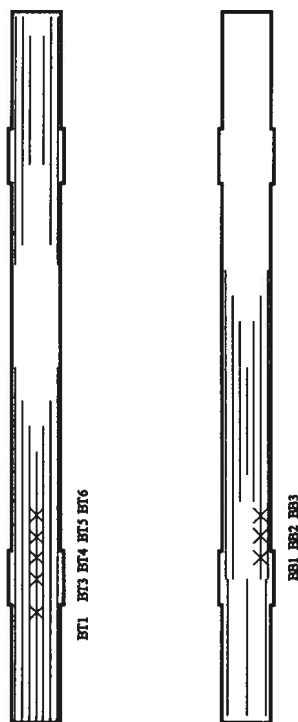


Fig. 4.4 Strain gauge locations (Plan). Elevation in Fig. 4.3

### 4.2.2. LVDT LOCATIONS

Three LVDTs were used to measure different displacements. First LVDT was installed 9' from the bottom of the specimen on the center line of the column parallel to the lateral loading plane to find the column tip deflections in the lateral loading direction. Although there is a built in LVDT in the lateral loading MTS jack the pin of that jack was

loose in the clevis of the loading plate. Therefore when the loading direction is reversed it was suspected that the load displacement relationship would not be very accurate.

The second LVDT was located 13.5" from the bottom of the specimen in the center line of the column. The third LVDT was located 3' 10.75" horizontally away from the second LVDT in the beam stub. See Fig. 4.5 and 4.6. The latter two LVDTs can be used to measure the crack widths in the beam stub, and the horizontal displacements in the joint and the beam stub.

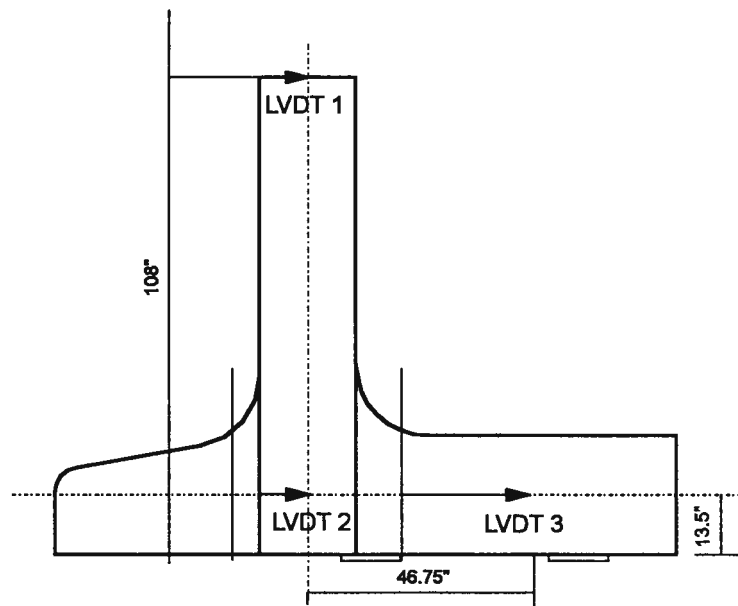


Fig. 4.5 LVDT locations

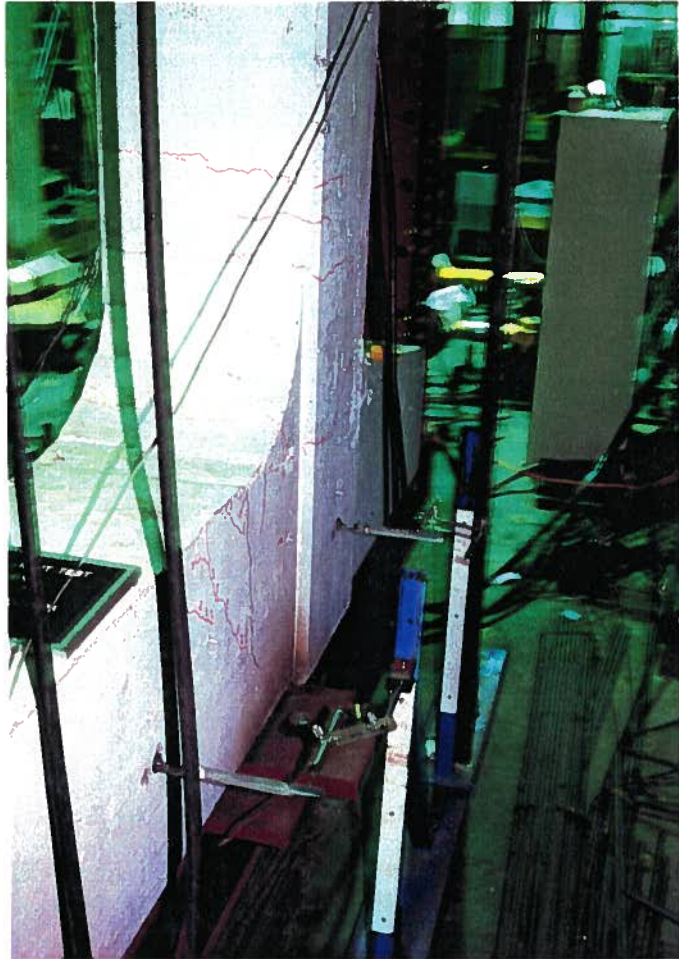


Fig. 4.6 Photo of LVDT locations

## **CHAPTER 5**

### **TESTING PROCEDURE**

#### **5.1 BOUNDARY CONDITIONS**

In the actual bridge the dead loads from the deck, to the bent are applied at the five girder positions. The lateral seismic load acts on the center of gravity of the deck which is 5' above the top of the bent. The lateral seismic load was assumed to be shared equally between the two, first interior bearings in the MOTH full bent test.

Two supports (bearings) were used for the half bent specimen. The "first interior" support is a pin to take the total lateral load, and the "middle" support is a roller so that it will share the vertical reaction due to the lateral seismic load with the pin support. These bearings consist of 2 steel plates of 2" and 1.5" thick and a 3/8" elastomeric pad between the plates. The bearing locations are shown in Figs. 5.1 and 5.2. The bearing arrangement is shown in the Fig. 5.3. The bolts attaching the top bearing plate to the bottom plate at the pin support is provided with 1/8" play so that the top bearing plate can rock on the elastomeric pad. At the roller support 1.5" slotted holes were drilled to allow for the horizontal movement of the specimen on the bearing pad. Figures 5.4 and 5.5 are photographs of pin bearing and, the vertical and horizontal jack connection detail.

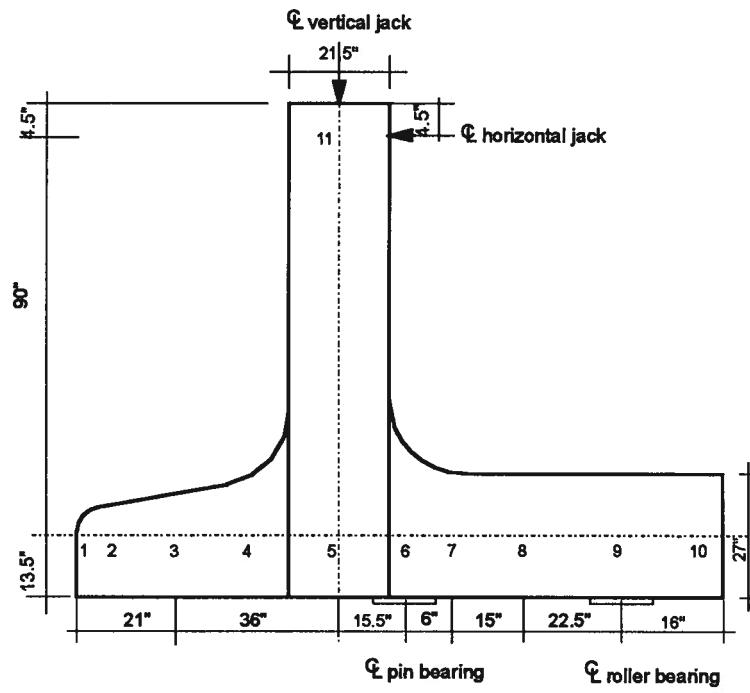


Fig. 5.1 Specimen OJ1 bearing locations



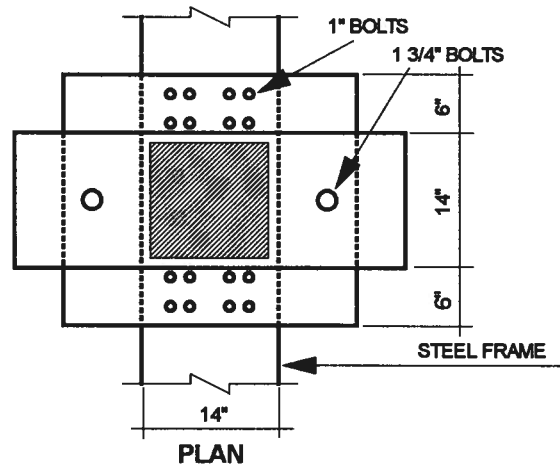
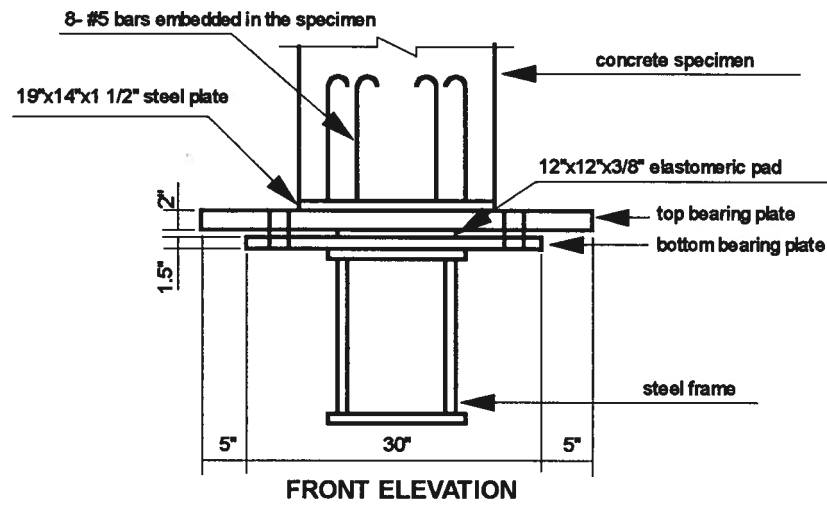


Fig. 5.3 Bearing arrangement

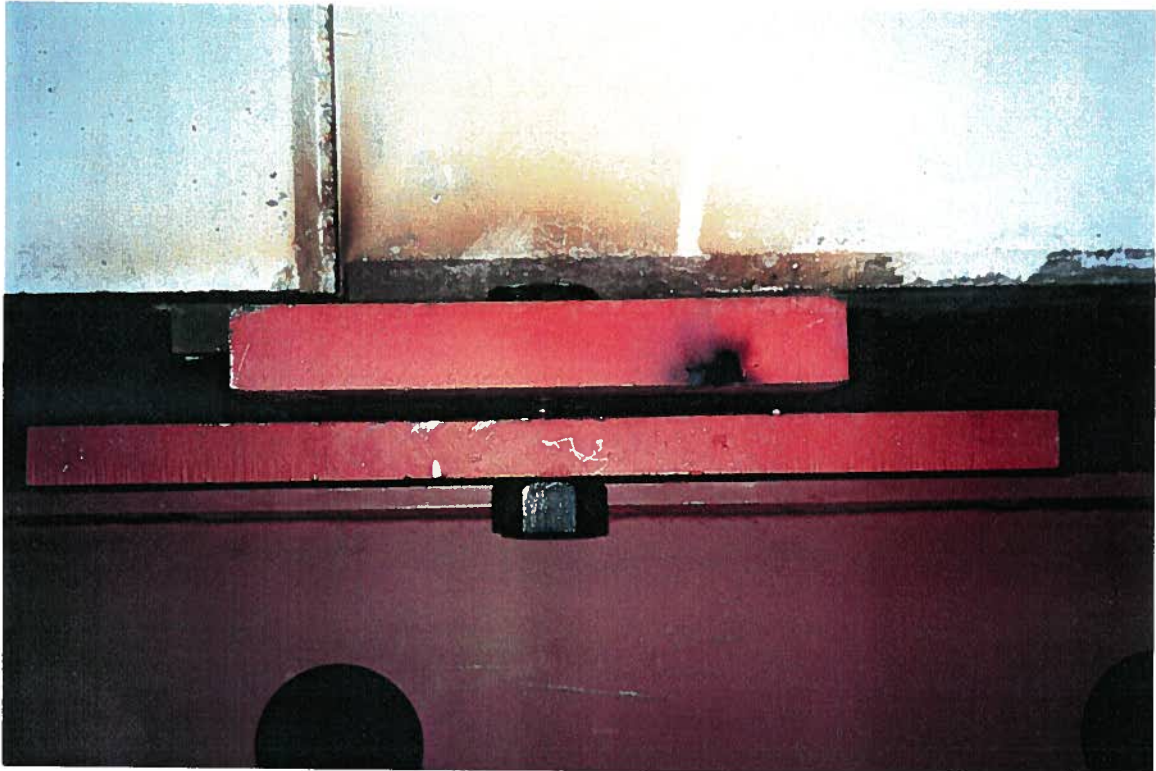


Fig. 5.4 Photograph of the pin bearing

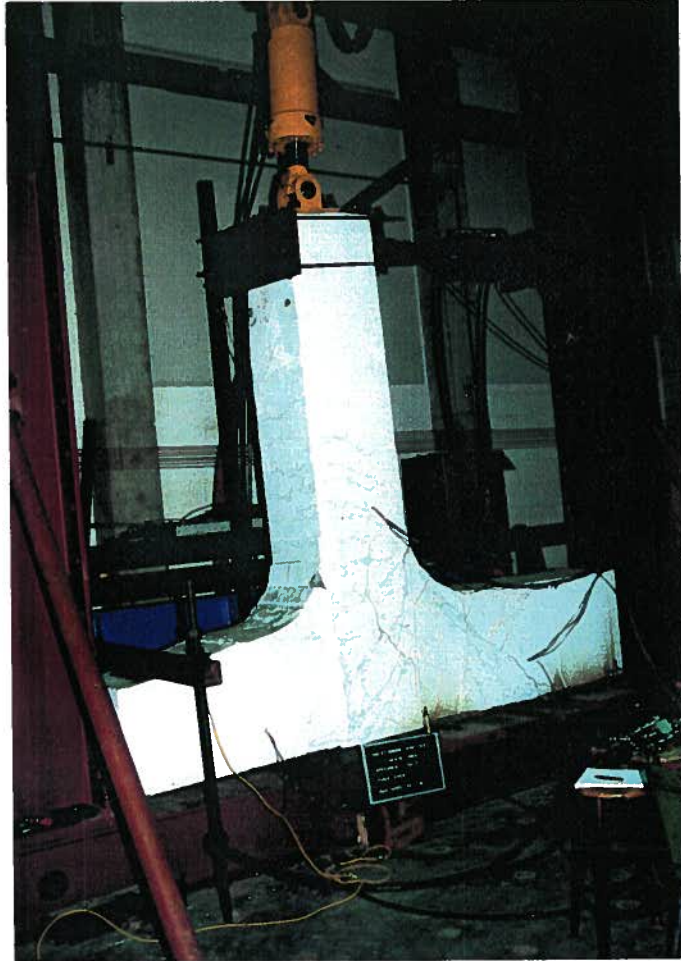


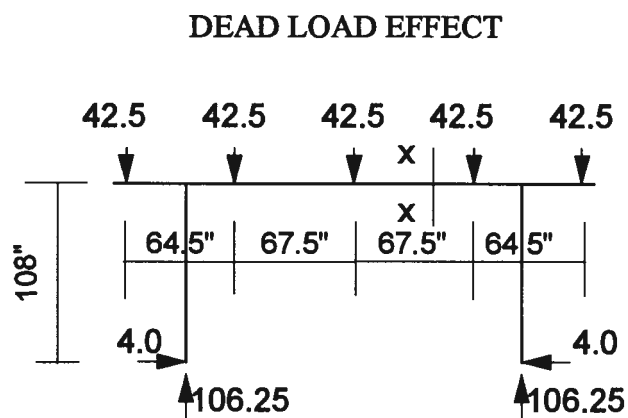
Fig. 5.5 Horizontal and vertical jack connection.

## 5.2 LOADING SEQUENCE

The shape of the load deflection curve and the energy dissipation capabilities depend on the loading path and history of cycles. Therefore it is important to apply similar loading patterns if comparison of results of different tests are expected to be carried out. Specimens subjected to large load reversals at the beginning of the load history show a significant deterioration of energy absorbing capacity, i.e. initial large displacements promotes deterioration of energy absorbing capabilities (Kawashima et al., 1988). For specimens which fail in shear, the number of inelastic loading cycles has a more significant effect than for flexural specimens. The number of loading cycles is important in flexural specimens if the ultimate failure mode is associated with the tension failure or bond failure of main bars (Koyama et al., 1988).

## 5.3 LOADING ON THE FULL BENT MODEL

In the Oak St. Bridge, dead load from the deck acts at the five bearing positions on the cap beam of the bent. The lateral load is assumed to act on the center of gravity of the deck which is 5' above the center line of the cap beam. Fig. 5.6 shows the forces and reactions due to dead and lateral loads acting on the MOTH full bent model. Section x-x is taken to the right of mid span of the cap beam. The lateral load is denoted  $P$  and is analogous to the seismic base shear. As the half bent specimens were tested upside down, the dead loads have been taken as 42.5 kips, reflecting the total dead load of the specimen including the column.



ALL LOADS ARE IN  
KIPS

P = LATERAL LOAD

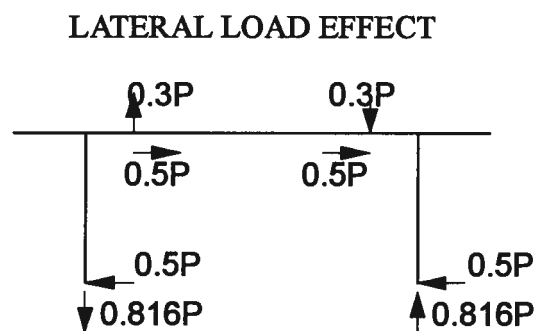
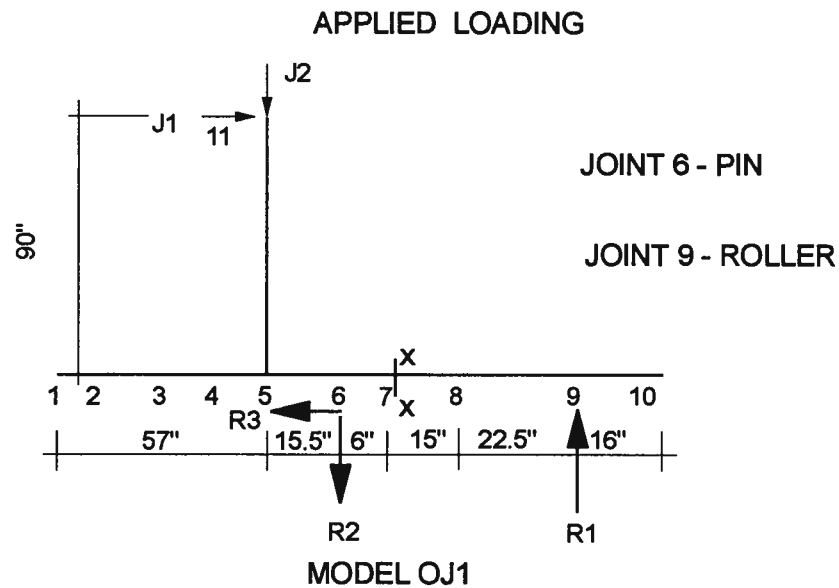


Fig 5.6 Dead and lateral loads on full bent test

#### 5.4 LOADING ON HALF BENT SPECIMEN OJ1

Specimen OJ1 was tested using 2 jacks at the tip of the column. The two jacks used for the application of the column reaction vertically (J2) and horizontally (J1) had a capacity of 200 kips and 100 kips respectively. The 200 kip jack is double acting with 12" stroke, whilst the 100 kip jack is double acting with 6" stroke. The 100 kip jack was used to apply slow reverse cyclic loading laterally at the column top under displacement

control, while the load of the vertical 200 kip jack was controlled proportionately to the 100 kip jack. The bending moment at the cap beam end (joint 10), corresponding to mid span in the full bent tests, has been neglected for both specimens OJ1 and OJ2 to simplify the loading arrangement, i.e. to reduce the number of jacks. Fig. 5.7 shows the load application on specimen OJ1. The line diagram shows member centerline dimensions. The first interior support, the pin, will absorb the total lateral load due to the earthquake and the vertical load due to the earthquake will be carried by the pin and the roller, such that the shear force of the cap beam at the roller is in the required region.



$$R1 = 2.07 J1 - 0.35 J2$$

$$R2 = 2.07 J1 - 1.35 J2$$

$$R3 = J1$$

Fig 5.7 Loading OJ1

From Fig. 5.6, shear at section xx (joint 7) due to dead load is -21.25 kips. Shear at xx due to live load is  $-0.516P$  kips. Where  $P$  is the lateral load acting on the MOTH full bent. Shear is taken as positive using the usual beam convention. The resulting total shear  $V$  at section xx, when  $P$  is positive acting to the right is,

$$V = -21.25 - 0.516P \quad (1)$$

For the half bent specimen the corresponding shear in the cap beam based on the geometry and support conditions of the specimen OJ1 (Fig. 5.7) is,

$$V = 2.07 (J1) - 0.35 (J2) \quad (2)$$

Jacks J1 and J2 were then controlled to obtain the variation of  $V$ . The sequence, maximum lateral displacement and the maximum lateral load applied at the column tip are given in Table 5.1. The jack J2 was controlled in relation to J1 according to the relationship in equation 3,

$$J2 = 2.17 (J1) + 47.23 \quad (3)$$

The corresponding J2 jack loads and the sequences are given in Table C1 of Appendix- C.

The Fig. 5.8 and 5.9 show the loading curves of J1, J2 and the variation of shear and bending moment at section xx of the specimen OJ1 cap beam. The axial load acting in the cap beam at this section is zero. The Fig. 5.10 shows the variation of shear at section xx in

the half bent test and the MOTH full bent (OSB1) with the loading sequence. The force resultants for the complete specimen OJ1 and OSB1 at the maximum loading condition are given in the Appendix B (Figs. B1-B8).

Table 5.1 Jack J1 displacement and min/max load

Sequence	Displ. J1 (in)	min(kips)	max(kips)
A	0.1	23.0	26.8
B	0.2	12.1	32.0
C	0.25	11.6	33.2
D	0.3	12.2	36.2
E	0.5	10.2	41.2
F	0.6	7.3	43.4
G	0.7	3.1	45.6
H	1.00	-2.1	51.0
I	1.25	-7.1	51.4
J	1.5	-13.9	47.2
K,L,O	2	-9.1	49.5
P	2.5	-15.6	41.6

Positive acting to right (see Fig. 5.7)

Initial load of the lateral jack was  $J1=22.5$  kips acting to the right hand side (Fig. 5.7) to obtain the dead load shear at the roller bearing of the cap beam. At this load lateral

column tip deflection was 1.4". This was the zero position for J1 displacement in Table 5.1.

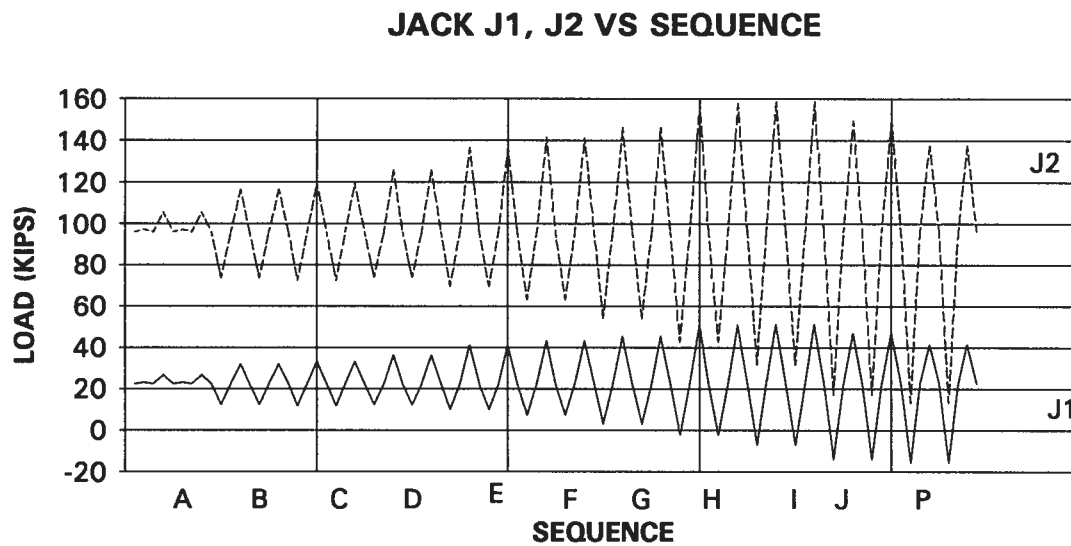


Fig. 5.8 Applied jack loads specimen OJ1

Shear and Moment Variation Vs Jack Loads

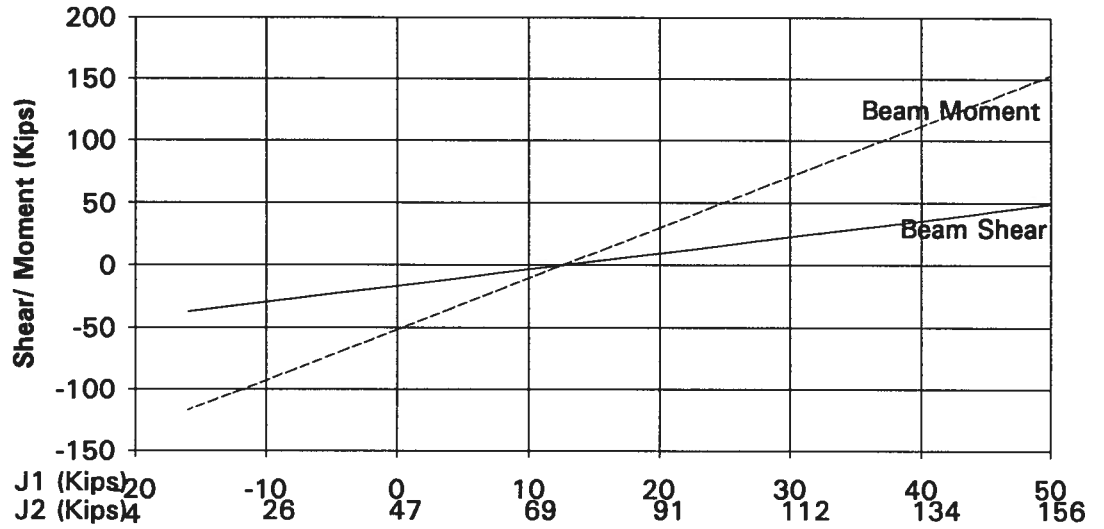


Fig. 5.9 Shear/Moment variation of OJ1 cap beam section xx with jack loads

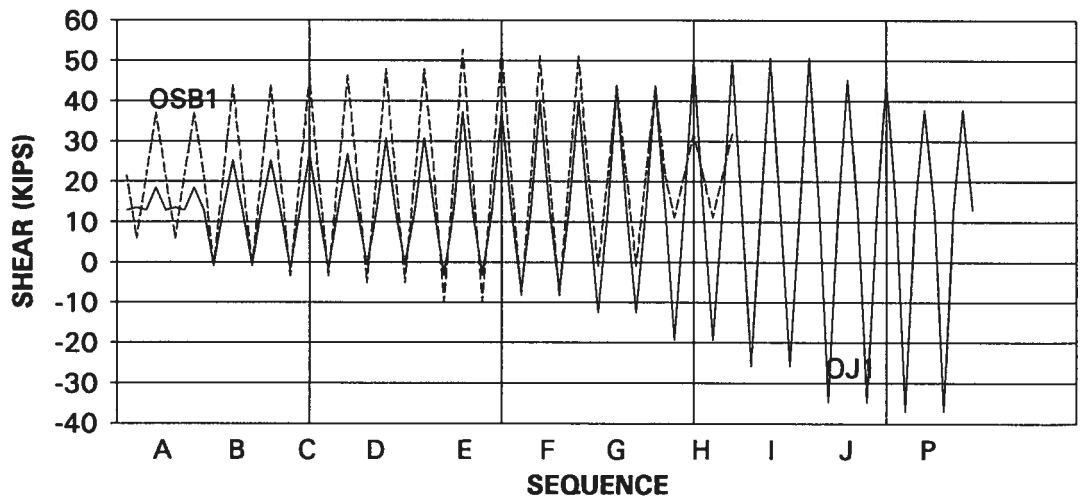


Fig. 5.10 Cap beam shear variation of specimen OJ1 and OSB1

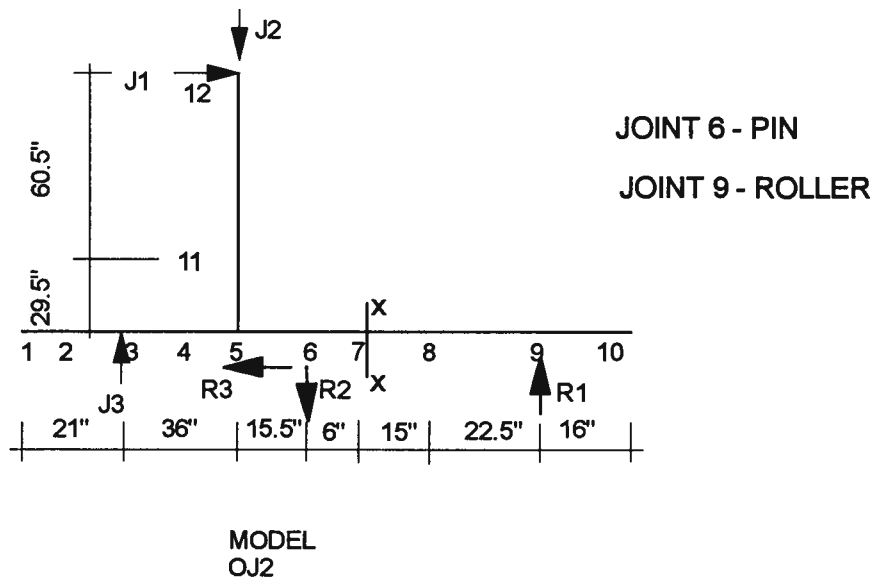
Fourteen sequences of sinusoidal lateral load cycles were applied during the first test but due to malfunction of the data acquisition system data for 2 of the sequences were not recorded. Each sequence consisted of two cycles. The period of the cycles were 10 minutes and the scan rate was 2 seconds. Due to the restriction of the stroke of the lateral jack maximum displacement applied was 2.5".

Upon completion of this test, the column remained undamaged. It was therefore decided to carry out a column test on the same specimen. A third support and a tie down on the cantilever side of the cap beam was provided. The two sides of the cap beam ends were supported against the steel frame. Three sequences of 1",2",2.5" displacements at the column tip was applied. The stroke to the north (pulling) was only 2.5", therefore it was decided to apply a push to the south with the maximum available stroke of 3.5".

## 5.5 LOADING ON HALF BENT SPECIMEN OJ2

The specimen OSB2 was retrofitted to improve the cap beam shear and moment capacity. This retrofit scheme consist of applying 210 kips of post tensioning force to the existing cap beam through a cored hole. The cap beam of the specimen OJ2 was externally post-tensioned by using 1.5" thick end plates and six 5/8" Dywidag bars each carrying 35 kips. These forces were applied to specimen OJ2 such that it will duplicate the post tensioning forces applied for the specimen OSB2.

In specimen OJ1 the major concern was cap beam shear. Therefore during testing of specimen 1 correct shear in the cap beam was applied using two jacks at the column tip. But in the retrofitted specimen column shear is also of major concern. Therefore the correct column reactions were applied at the tip of the column using J1 and J2, and a third jack (J3) was controlled to obtain the correct shear in the cap beam. Loads in both vertical jacks were allowed to change in proportion with the lateral jack. The lateral jack was on reversed cyclic loading under displacement control. The third jack J3 was 3' away from the joint 5 on the cantilever side.(Fig.5.11)



$$R1 = 2.1J1 + 0.8J3 - 0.4J2$$

$$R2 = 2.1J1 + 1.8J3 - 1.4J2$$

$$R3 = J1$$

Fig. 5.11 Loading OJ2

The two jacks at the column tip J1 and J2 were varied in relation to P (lateral load on the MOTH full bent) to obtain similar column loading to the Full bent test,

$$J1 = P/2+4 \quad (4)$$

$$J2 = 0.816 (P) + 106.25 \quad (5)$$

$$J3 = 42.5 - 0.24P \quad (6)$$

The third jack J3 was varied such that the cap beam shear at section xx is (Section 5.4),

$$V = -21.25 - 0.516P \quad (7)$$

Jacks J1, J2 and J3 were controlled to obtain the variation of shear both in the column and the cap beam. The sequence, maximum lateral column tip displacement and the maximum lateral load (J1) applied at the column tip are given in the Table 5.2. The other two jacks J2 and J3 were controlled in relation to J1. The corresponding J2 and J3 jack loads are given in Table C.2 of Appendix C. The Figs. 5.12, 5.13 show the loading curves of the three jacks and the variation of shear and the moment at beam section 7 and column section 11 (Fig.5.11) of the specimen OJ2. The axial load at section 7 of the cap beam is zero. The Fig. 5.14 and 5.15 show the comparison of the variation of the shear of OJ2 and OSB2 at the section 7 of the cap beam and the column respectively. The force resultants for the complete specimen OJ2 and OSB2 at the maximum loading condition are given in the Appendix B (Figs. B9-B16).

The initial load of J1 for the second test was  $J1=4$  kips acting to the right hand side to account for the dead load reaction at the column tip. The other two jacks were varied according to equations (5) and (6). Thus at  $J1=4$  kips,  $J2=106.25$  kips, and  $J3=42.5$  kips. This simulates the dead load condition.

Table 5.2 Jack J1 displacement and min/max load

Sequence	Displ. J1 (in)	min (kips)	max (kips)
A	0.1	-1.1	6.3
B	0.2	-5.8	8.7
C	0.4	-12.5	19.8
D	0.6	-19.4	29.3
E	0.75	-24.5	35.8
F	1.00	-32.8	43.4
G	1.25	-38	49.2
H	1.50	-40.2	51.3
I	1.75	-41	50.5
J	2.00	-41	50.2
K	2.50	-42.9	60.6
L	3.00	-42.3	56.4
M	4.00	-45.6	30.8

Positive acting to right (see Fig. 5.11)

Thirteen sequences of load cycles were applied. Due to the malfunction of the column tip LVDT 3 sequences had to be repeated. The number of cycles per sequence, period and the scan rate were similar to the specimen OJ1. In the sequence J (2" lateral displacement) for pulling the stroke was not enough. Therefore a 0.5" steel plate was inserted underneath the roller to get an extra 1" displacement at the column tip. After that another two sequences of 2.5" and 3" were applied. Then the steel plate was removed and

a push of 4" was applied. The last three sequences were recorded in the Table 5.2 for completeness. But those were not taken in to account for subsequent calculations because they look unreliable.

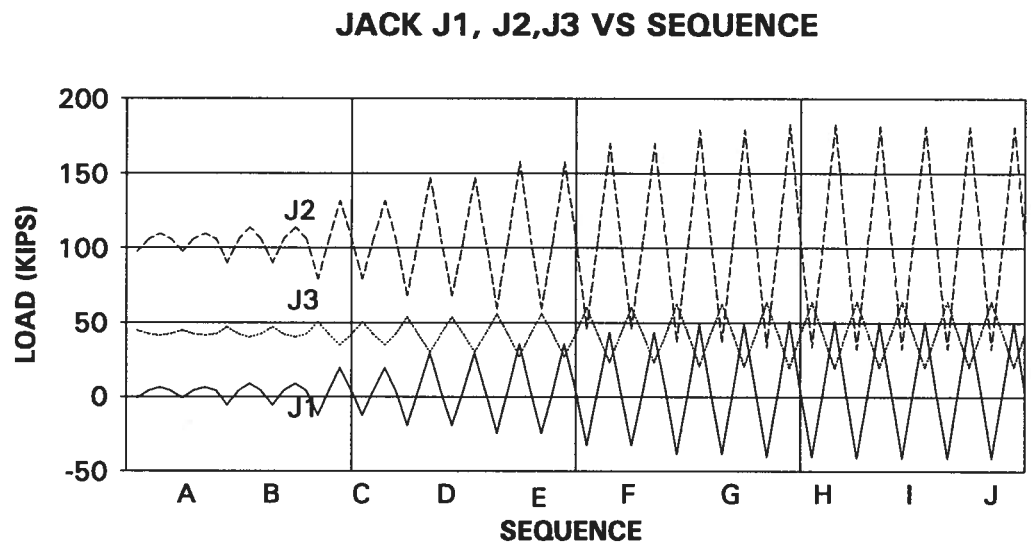


Fig. 5.12 Applied jack loads specimen OJ2

**Shear and Moment Variation Vs Jack Loads**

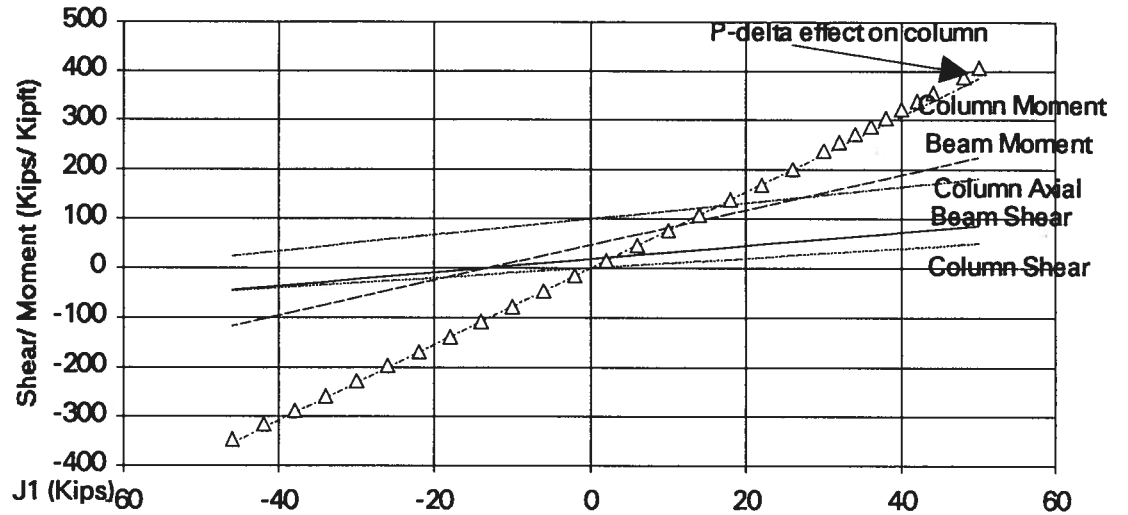


Fig. 5.13 Shear /Moment variation at x-x of OJ2 with jack loads

**CAPBEAM SHEAR VS SEQUENCE**

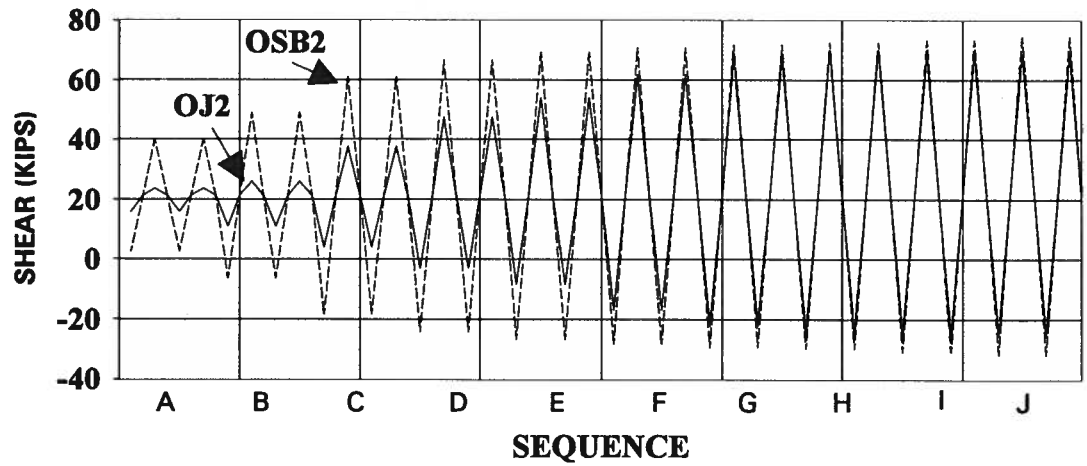


Fig. 5.14 Cap beam shear variation of specimen OJ2 and OSB2

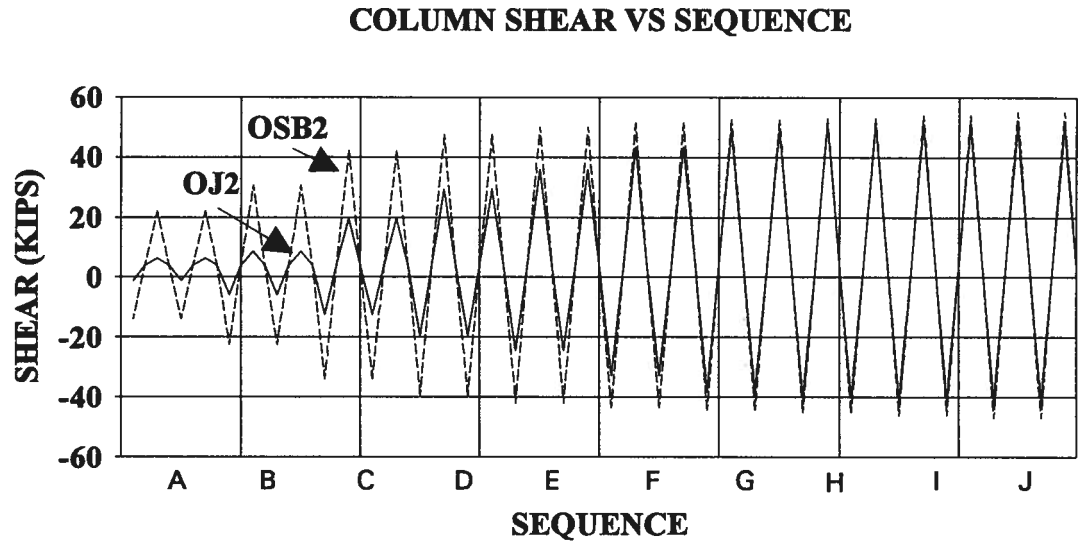


Fig. 5.15 Column shear variation of specimen OJ2 and OSB2

## CHAPTER 6

### EXPERIMENTAL OBSERVATIONS

#### 6.1 SPECIMEN OJ1

##### 6.1.1 OBSERVED BEHAVIOUR

Flexural cracks in the column (south side ) appeared when pulling to the north in sequence A at 0.1" displacement. These cracks extended in the subsequent cycles. In sequence E at 0.5" displacement (pulling) and a lateral load (J1) of 41.2 kips first flexural cracks at the top side (bottom on the upside down specimen) of the cap beam appeared. These cracks extended in the subsequent sequences. Fig. 6.2 shows the cracks of sequence F at 0.6" lateral column tip displacement. At sequence F the lateral load J1 applied was 43.4 kips and the cap beam shear at section xx (Fig. 5.7) was 40.3 kips. The peak lateral load was obtained in sequence H at 1" column top displacement. At this sequence the width of the cap beam shear crack was about 0.6mm. Up to sequence J (i.e. 1.5" column tip deflection) when loading north (pulling) the cap beam top shear crack opened up without forming other cracks. After sequence H the strength and the stiffness of the specimen started degrading. This can be clearly seen from the lateral load displacement hysteresis loops of the column tip (Fig. 6.1). The initial position of the lateral loading jack for this test was 1.4". In sequence O at 2" lateral column tip deflection (Fig. 6.3) a major shear crack started spreading in the joint region when pushing South. At this sequence the lateral load applied was 49.5 kips and the cap beam shear at section xx was 48.3 kips. The

width of the cap beam top shear crack was about 8 mm in this sequence. The lateral load dropped to 41.6 kips in sequence P at a displacement of 2.5"(Fig. 6.4 ).

As explained in the section 5.4 (by using an extra support and a tie down on the cantilever side of the cap beam), a separate column test was carried out with four load sequences. The load displacement curve of this test is shown in the Fig. 6.5 and the cracking at the last sequence is shown in the Fig. 6.6. In these sequences there was no major cracking in the column apart from the extension of the cracks that were already formed. Hysteresis loops of the column test clearly shows the yielding of column steel in both directions (Fig. 6.5).

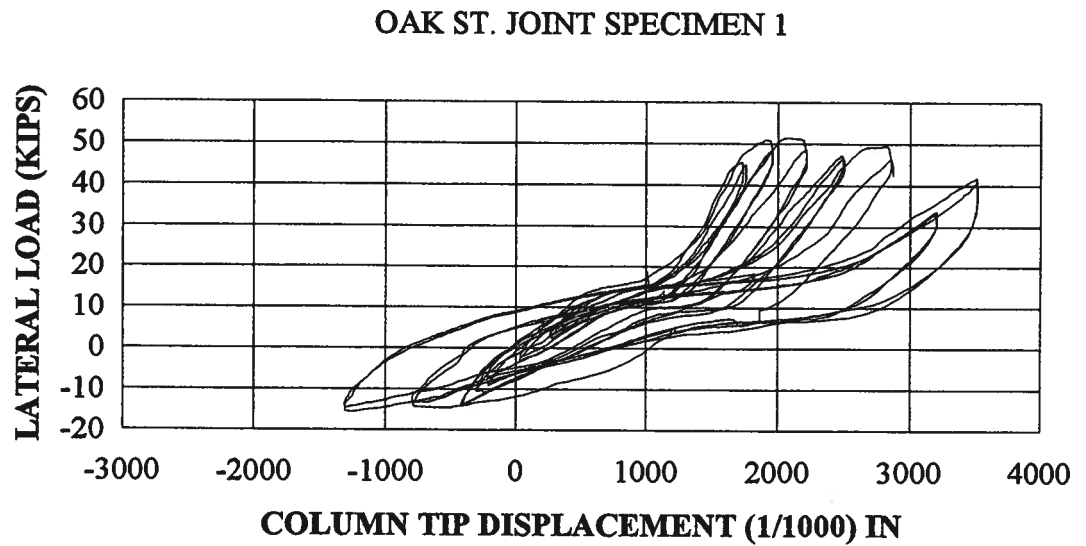


Fig 6.1 OJ1 Load displacement at the column tip

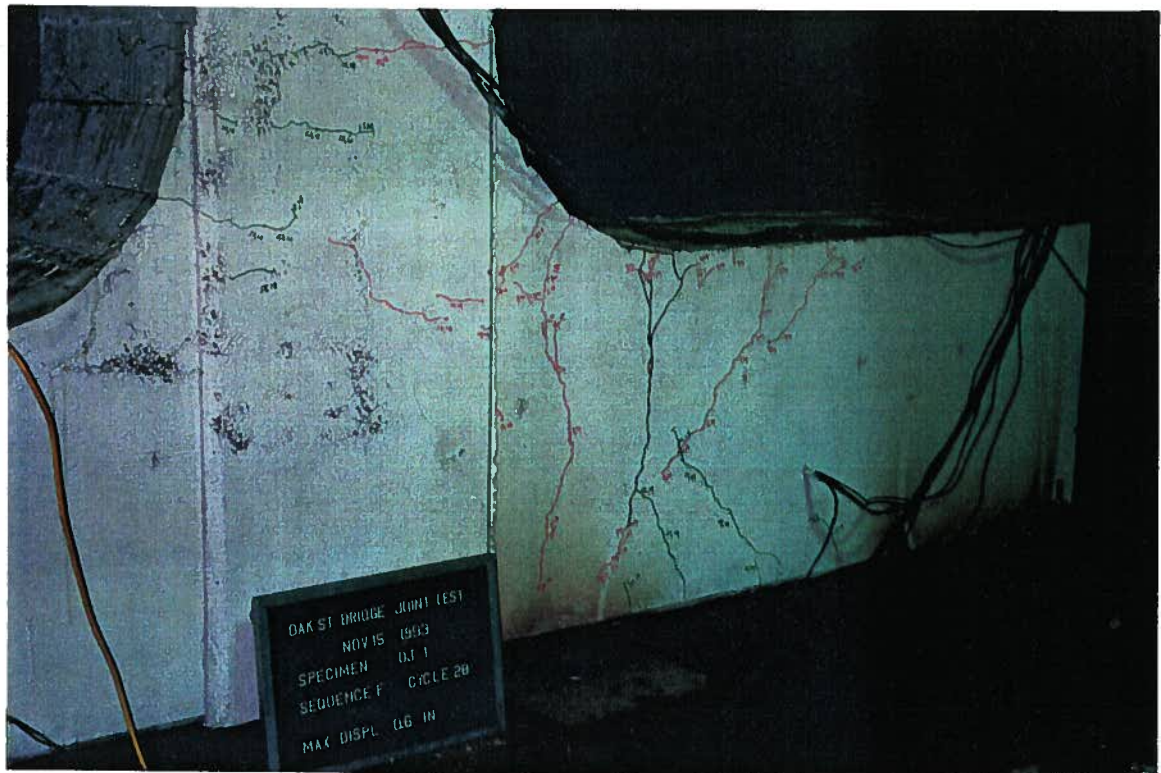
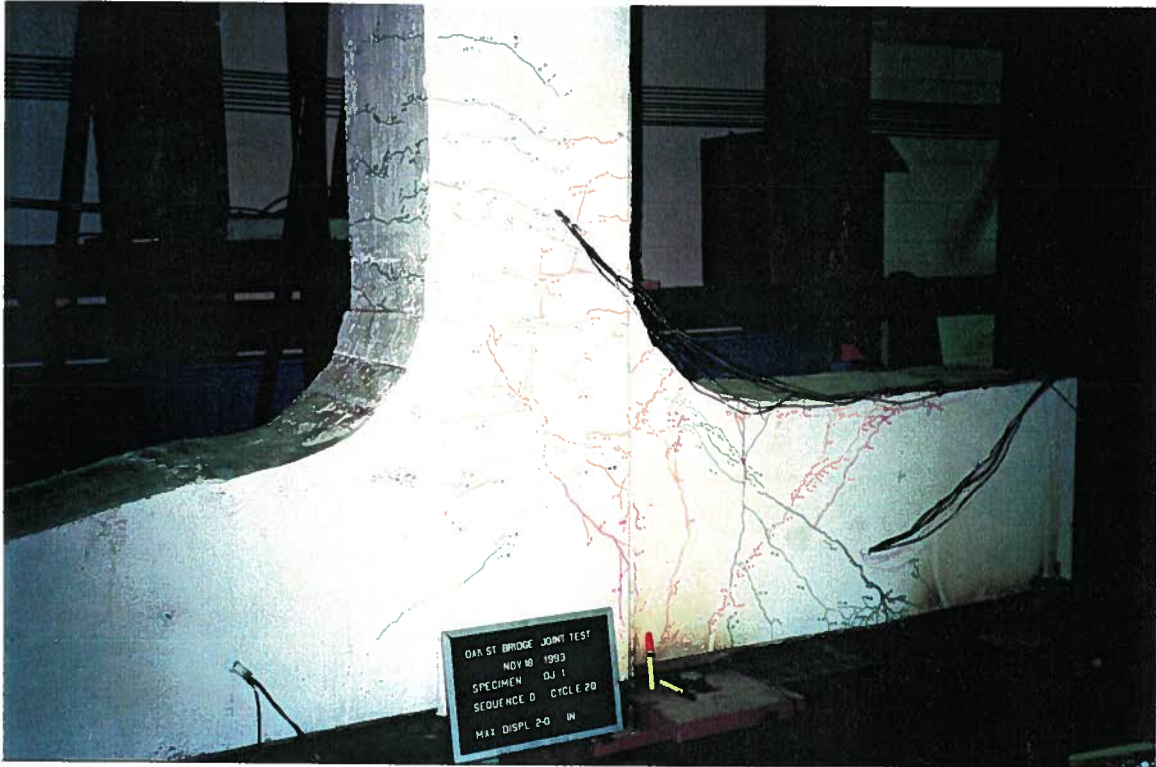
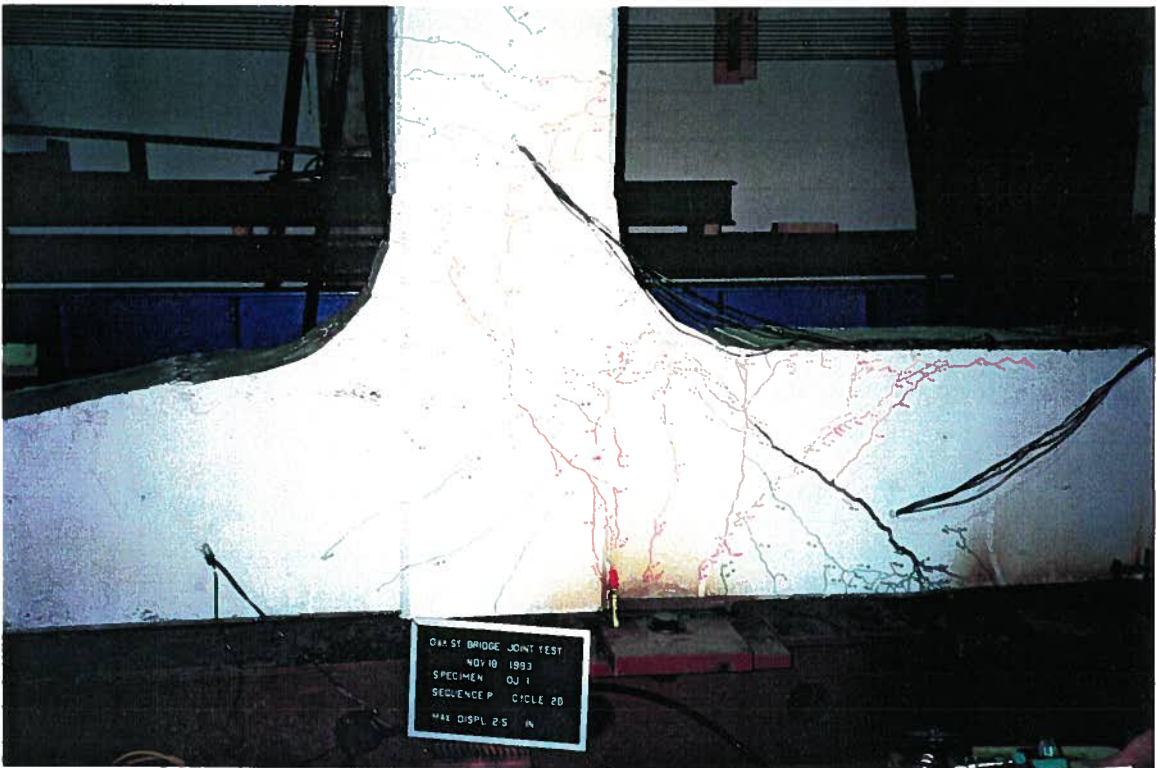


Fig. 6.2 Photograph of crack patterns at sequence F



**Fig. 6.3** Photograph of crack patterns at sequence O



**Fig. 6.4** Photograph of crack patterns at sequence P

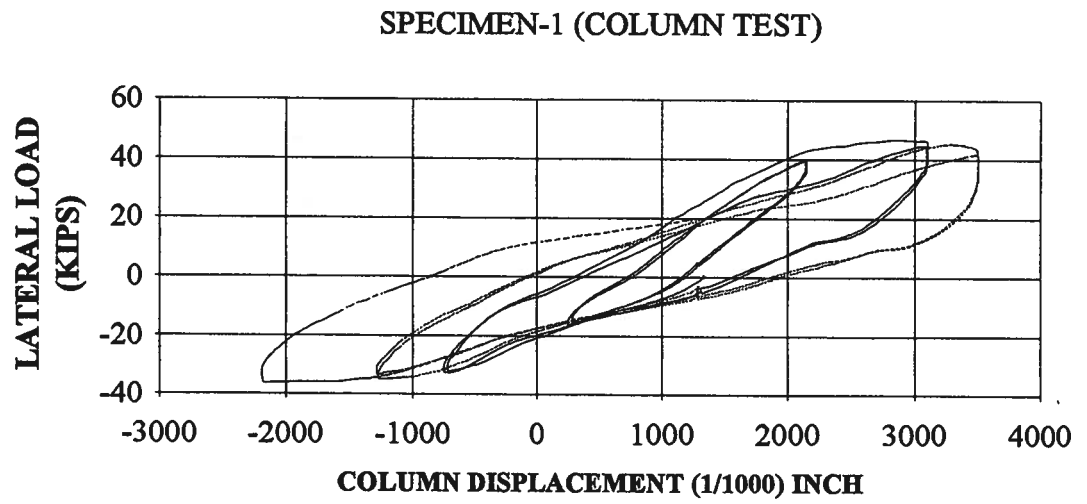


**Fig 6.5 Load displacement at the column tip (Column Test)**

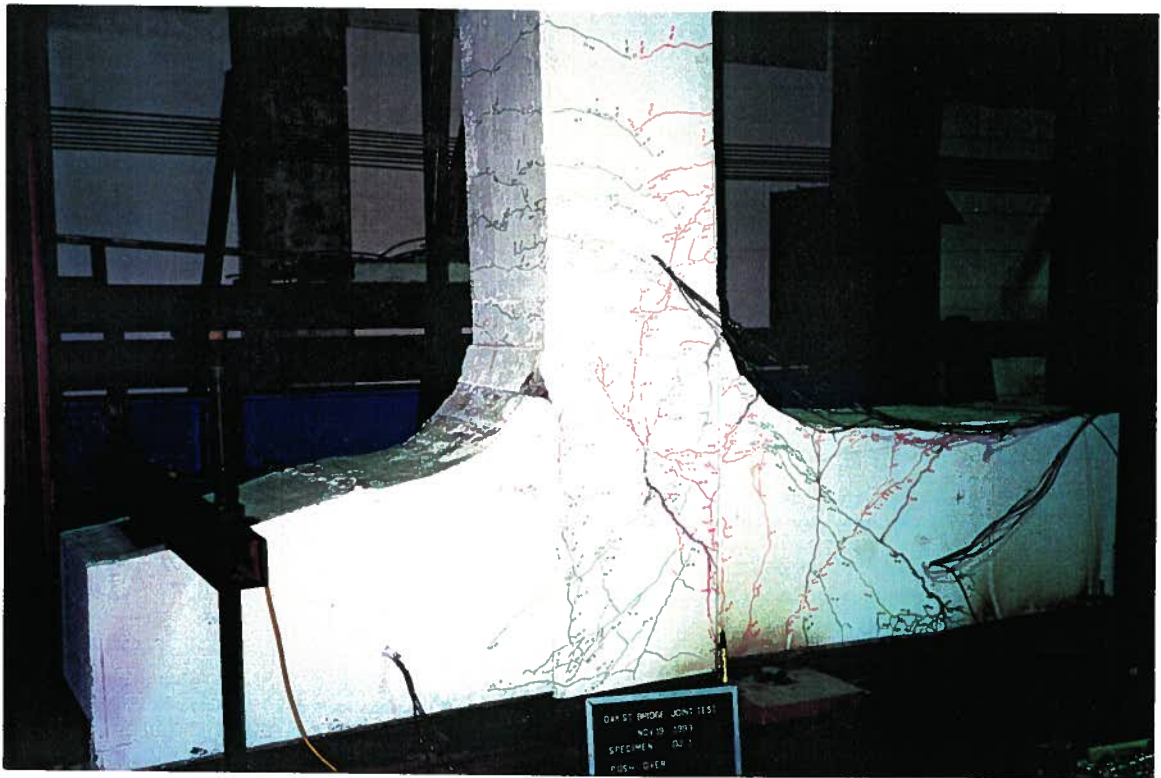


**Fig. 6.6 Photograph of crack patterns at Push Over**

### 6.1.2 SECTIONAL ANALYSIS

The maximum sectional forces and sectional capacities of specimen OJ1 are compared in this section at locations where plastic hinges or shear failure were anticipated. Node locations and load application are shown in Fig. 5.7. The applied cap beam moment and shear force variations were given in Fig. 5.9. Appendix B describes the force resultants of the whole specimen at the maximum load.

Table 6.1 OJ1 Maximum demand (critical sectional forces) for pulling

MEMBER	NODE	AXIAL FORCE (kips)	SHEAR FORCE (kips)	MOMENT (kip ft)
10 (column)	5	159.0	51.4	385.5
	11	-159.0	-51.4	0.0
6	6	0.0	-49.7	-180.1
	7	0.0	49.7	155.3
7 (section x-x)	7	0.0	-49.7	-155.3
	8	0.0	49.7	95.0

Table 6.2 Maximum demand (critical sectional forces) for pushing

MEMBER	NODE	AXIAL FORCE (kips)	SHEAR FORCE (kips)	MOMENT (kip ft)
10 (column)	5	12.5	-16.0	-120.0
	11	-12.5	16.0	0.0
6	6	0.0	42.2	156.1
	7	0.0	-42.2	-127.5
7 (section x-x)	7	0.0	42.2	127.5
	8	0.0	-42.2	-77.3

The capacities at joint 7 (Fig. 5.7) were obtained using Program Response. Program Response was developed at the University of Toronto (Collins et al., 1991) to calculate concrete section capacities. The input consists of the sectional properties and the loading. The loading can be given as the axial load and the moment at zero shear and the variation of these two parameters with the shear. Using the applied loads at joint 7 of specimen OJ1, input values were obtained as shown in Table 6.3. Where, N is axial load, M is moment, and V is shear.

Table 6.3 Input loading OJ1 joint 7

	Specimen OJ1 Joint 7
Axial (kips) @ V=0	1.1
Moment (kip ft) @ V=0	2.48
dN/dV	0
dM/dV	3.07

The above input can be used to find out the influence of moment, axial load and the shear force on the section under consideration. The maximum shear obtained and the corresponding moment and the axial load at the joint 7 are shown in Table 6.4.

Table 6.4 Out put capacities OJ1 joint 7

	Specimen OJ1 Joint 7
Axial (kips)	1.1
Shear (kips)	61.1
Moment (kip ft)	190.1

These values were compared with the values obtained from the testing. The applied maximum forces for specimen OJ1 at joint 7 (Fig. 5.7) were 49.7 kips shear and 155.3 kipft moment (Table 6.1) The values predicted by the Program Response were 61.1 kips shear and 190.1 kipft moment (Table 6.4). Response predicted shear capacities were about 20% higher than the peak applied shear force, based on analysis only at joint 7.

### **6.1.3 STRAIN GAUGE READINGS**

The reinforcing bar yield stress is 345 MPa. Therefore yield strain should be around 0.001750 (1750 Micro strain). Surprisingly most of the beam stirrup strain gauges of specimen 1 close to the shear crack and column tie strain gauges of specimen 2 close to the flexural crack indicated very low strain values, (i.e. around 50 micro strain) in both tests. When there are cracks propagating across reinforcing bars then those bars are expected to carry most of the load if not all. Therefore the stirrup and tie strain gauge values are questionable. Bottom bar strain gauge BB3-12 of specimen 1 (Fig. 6.7) is clearly yielding in the last couple of cycles when pulling North. The other strain gauges of beam main bars also carried very high strains in the last couple of cycles i.e. BB2-11, BT5-5, BT6-6.

SPECIMEN 1 BEAM BOTTOM STRAIN GAUGE (BB3-12)

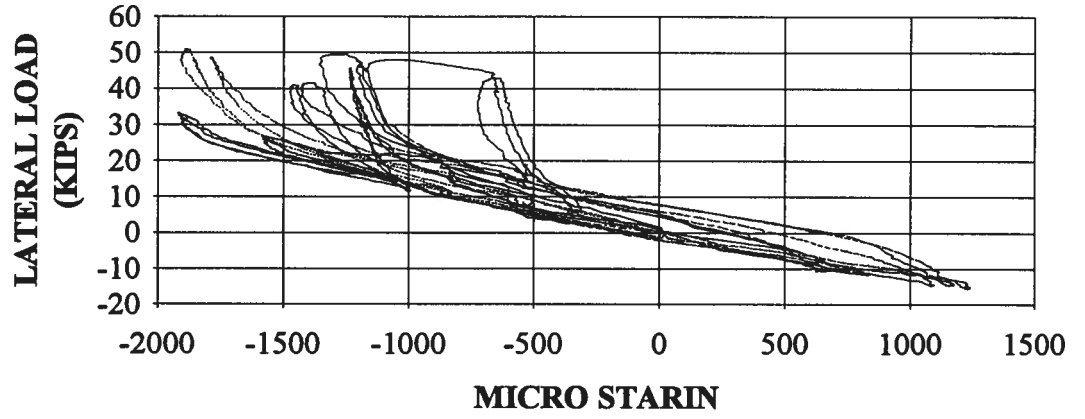


Fig 6.7 Strain gauge BB3

## **6.2 SPECIMEN OJ2**

### **6.2.1 OBSERVED BEHAVIOUR**

Flexural cracks in the column started in the sequence D (Fig. 6.9) at 0.6" lateral deflection of the column tip around 29 kips lateral load. At a lateral column tip displacement of 1" in the sequence F more flexural cracks in the column appeared. At this stage spacing of cracks in the column in both directions were around 6". This was very close to the spacing of the ties in the column which is 5 3/8". Flexural cracks in the cap beam appeared in sequence G at 1.25" lateral deflection of the column tip around 50 kips lateral load. At sequence H diagonal shear cracks in the column started to develop. This was at 1.5" lateral deflection of the column tip. As the test was started with an initial offset so that the correct dead load effects can be imposed, there was only 2" stroke in the North direction pulling. Therefore it was decided to insert a 0.5" steel plate at the roller bearing along with the neoprene pad to give an extra 1" of northward stroke to the lateral column tip jack. In sequence L (Fig. 6.10) at a lateral column tip deflection of 3" and a lateral load of 56 kips, the column flexural cracks just above the beam curve opened widely. At sequence M when the column tip deflection was 4" the column concrete started spalling.(Fig. 6.12).

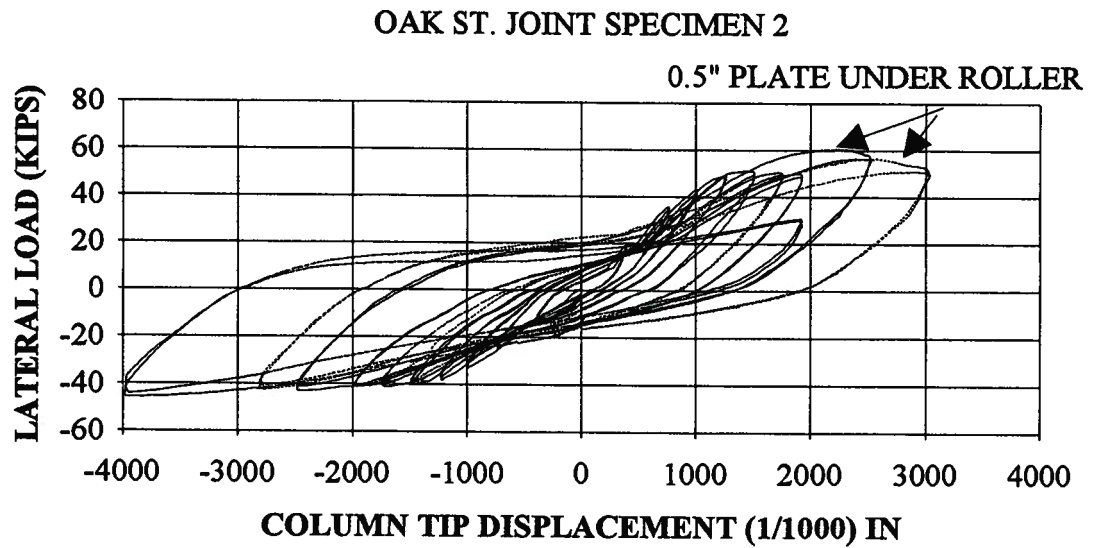


Fig. 6.8 OJ2 Load displacement at the column tip

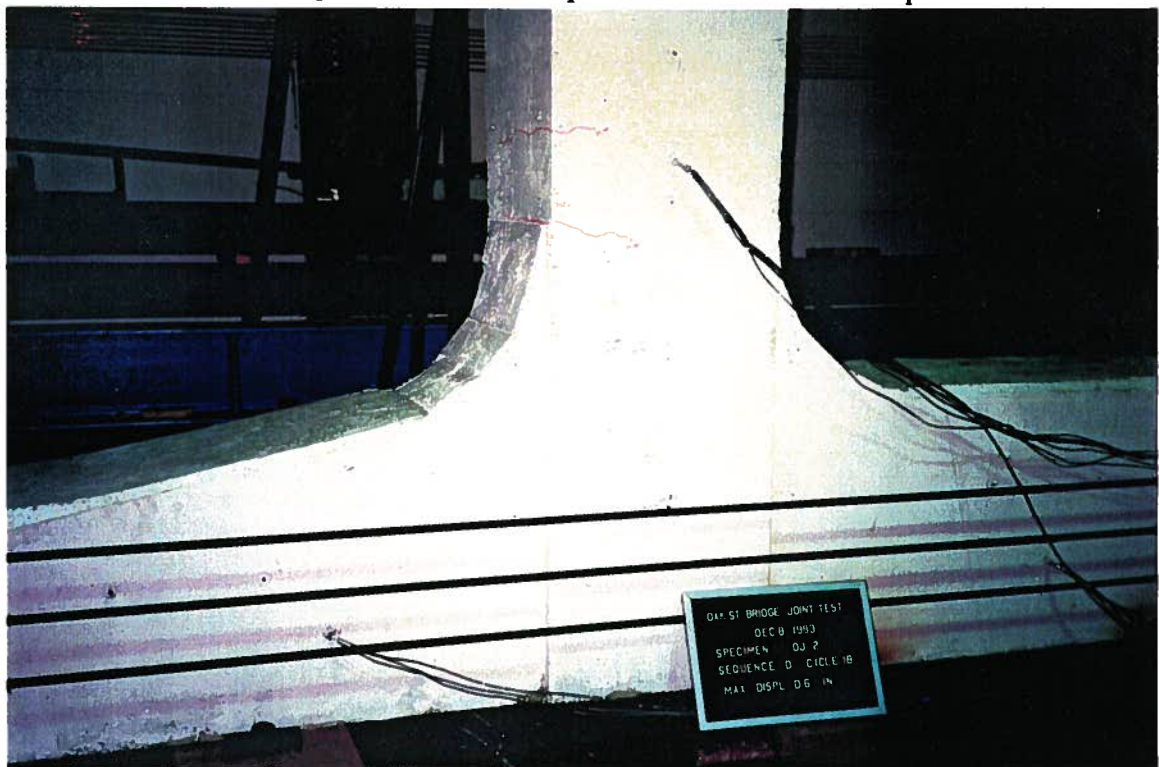


Fig. 6.9 Photograph of crack patterns at sequence D

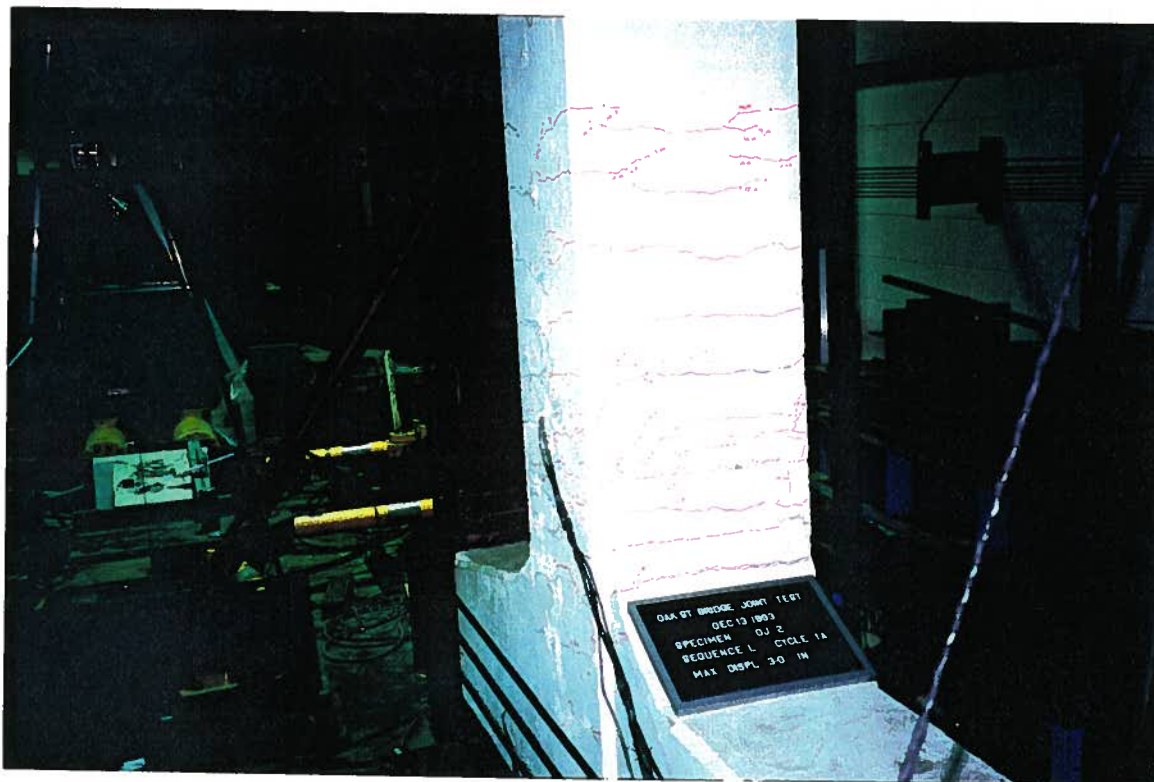


Fig. 6.10 Photograph of crack patterns at sequence L

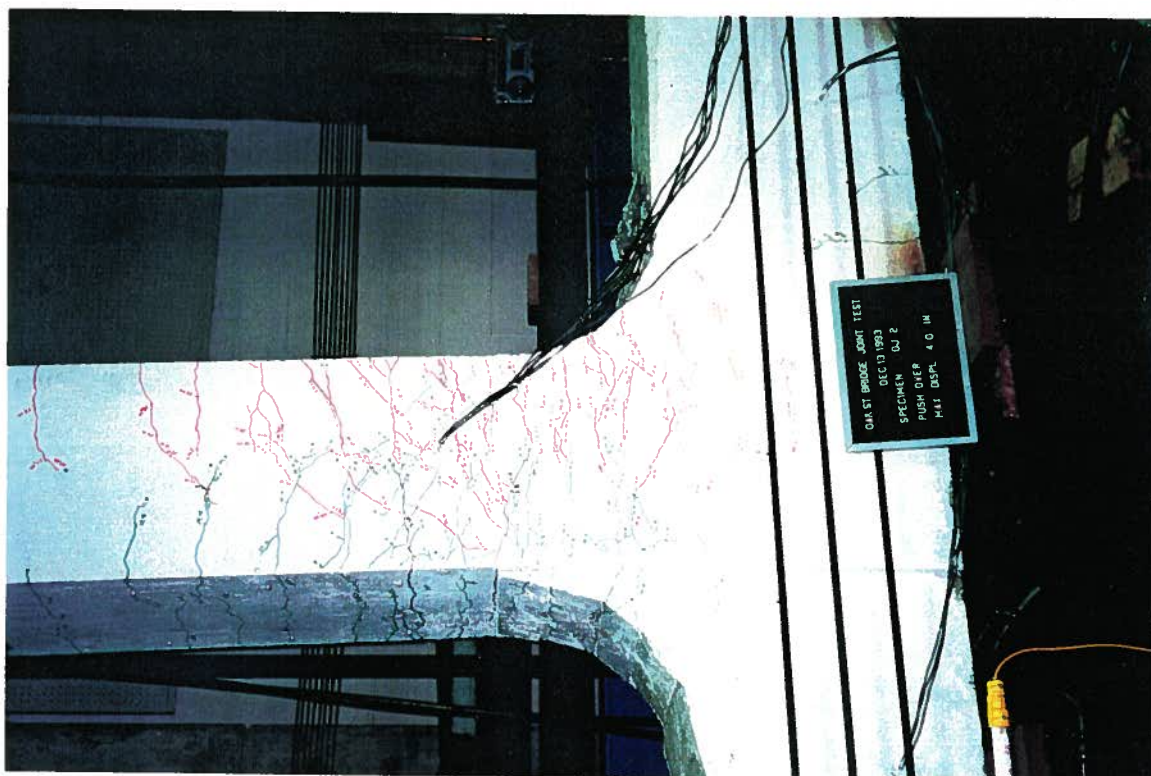


Fig. 6.11 Photograph of crack patterns at Push Over

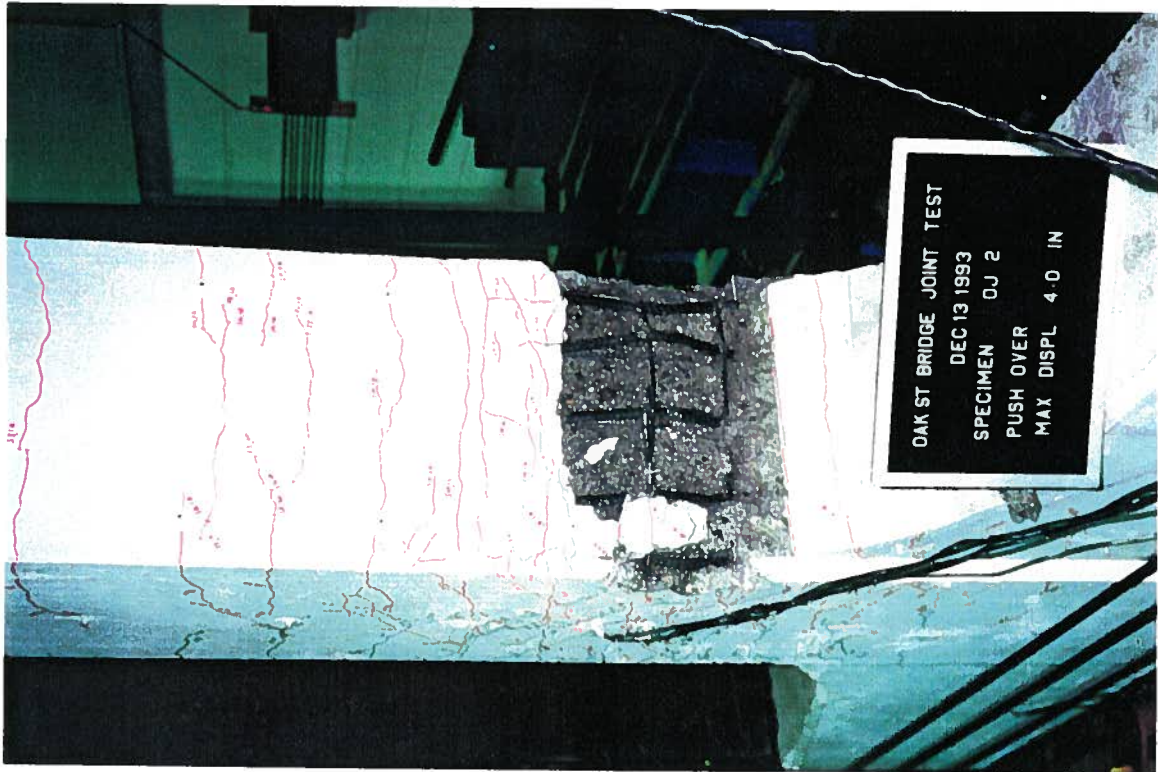


Fig. 6.12 Photograph of crack patterns at Push over

## 6.2.2 SECTIONAL ANALYSIS

The maximum sectional forces (the last 3 sequences were ignored because they appear to be unreliable) and sectional capacities of specimen OJ2 are compared in this section similar to specimen OJ1 at locations where plastic hinges or shear failure were anticipated. Node locations and load application are shown in Fig. 5.11. The applied cap beam and column force variations were given in Fig. 5.13. Appendix B describes the force resultants of the whole specimen at the maximum load.

Table 6.5 OJ2 Maximum demand (critical sectional forces) for pulling

MEMBER	NODE	AXIAL FORCE (kips)	SHEAR FORCE (kips)	MOMENT (kipft)
11 (column)	11	180.5	50.5	378.8
	12	-180.5	-50.5	0.0
6	6	0.0	-67.4	-244.3
	7	0.0	67.4	210.6
7 (section x-x)	7	0.0	-67.4	-210.6
	8	0.0	67.4	126.4

Table 6.6 OJ2 Maximum demand (critical sectional forces) for pushing

MEMBER	NODE	AXIAL FORCE (kips)	SHEAR FORCE (kips)	MOMENT (kipft)
11 (column)	11	26.3	-45.0	-337.5
	12	-26.3	45.0	0.0
6	6	0.0	32.5	119.8
	7	0.0	-32.5	-97.7
7 (section x-x)	7	0.0	32.5	97.7
	8	0.0	-32.5	-59.2

As explained in the section 6.1.2 of specimen OJ1 the input values at two critical sections of specimen OJ2 were calculated to be used in the Program Response (Collins et al.,1991). N is axial load, M is moment, and V is shear. The cap beam positive reinforcement had numerous cutoff points. Table 6.8 shows only the results for joint 7 and 11.

Table 6.7 Input loading OJ2 joints 7 and 11

	Specimen OJ2 Joint 7	Specimen OJ2 joint 11
Axial (kips) @ V=0	-210	-100
Moment (kip ft) @ V=0	-3.09	0
dN/dV	0	1.6
dM/dV	3.74	5.42

The calculated values of the maximum shear at joints 7 and 11 and the corresponding moment and the axial load values are shown in the Table 6.8.

Table 6.8 Output capacities OJ2 joints 7 and 11

	Specimen OJ2 Joint 7	Specimen OJ2 Joint 11
Axial (kips)	-210	38.5
Shear (kips)	82.2	38.5
Moment (kip ft)	304.4	208.4

Maximum push applied on specimen OJ2 at joint 11 (Fig.5.11) were 45 kips shear and 337.5 kip ft moment (table 6.6) The values predicted by the program Response were 38.5 kips shear at a Moment of 208.4 kip ft. The increase in the cap beam shear of the specimen OJ2 over OJ1 was around 35% without any significant cracking in the cap beam.

### 7.2.3 STRAIN GAUGE READINGS

In the specimen OJ2 column outside strain gauge CO4-29 (Fig. 6.13) yields when pulling North with 45 kips. The inside strain gauge CI3-23 (Fig. 6.14) yields when pushing south in the last couple of cycles. These high strain values clarifies the very high bending moments expected at specimen cross sections along these strain gauges. Strain gauges BB2-11 and BB3-12 of specimen OJ2 carries much lower strains than BB2-11 and BB3-12 of the specimen OJ1. This was due to the prestressing force applied to the cap beam of specimen OJ2.

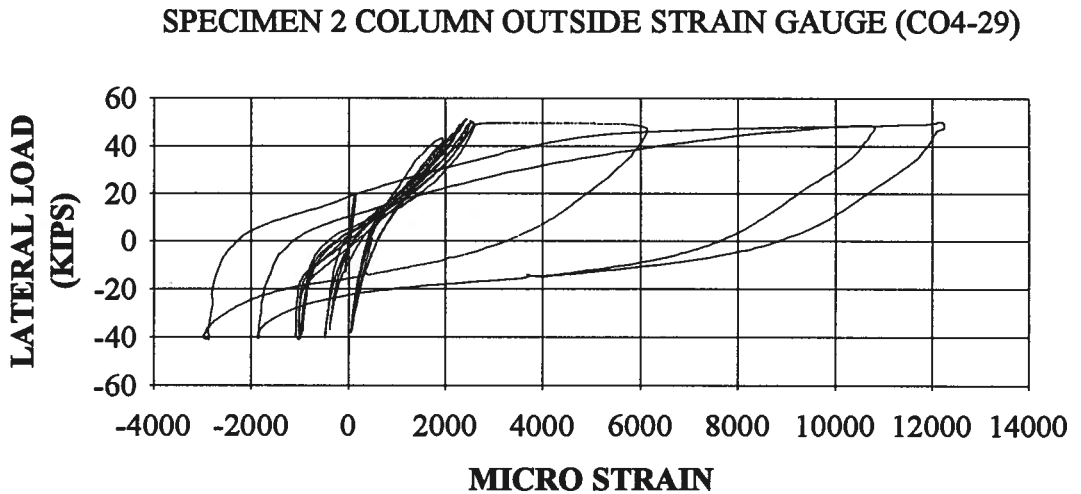


Fig 6.13 Strain gauge CO4

SPECIMEN 2 COLUMN INSIDE STRAIN GAUGE (CI3-23)

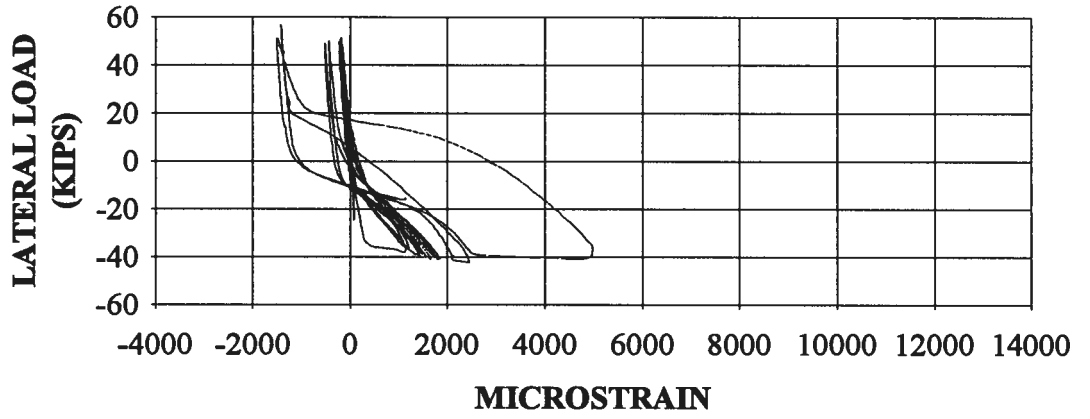


Fig 6.14 Strain gauge CI3

### 6.3 COMPARISON WITH BENT TEST RESULTS

Fig. 6.15 shows hysteresis loops from test OSB2. The displacement at the column tip of specimen OJ2 at  $\mu=1$  was 1.25" and the displacement of OSB2 at the joint for the same level of ductility was around 0.3". This difference is partly due to the simplified boundary conditions of the specimen OJ2. i.e. the roller bearing of the specimen OJ2 will stop the vertical movement of the cap beam at that location and also the bearings did not function as expected. The pin allowed the specimen to slide a little instead of allowing rotation. This can be seen in the load displacement curve of specimen OJ2 (Fig.6.8) by the sudden change in stiffness close to zero displacement in both pulling and pushing.

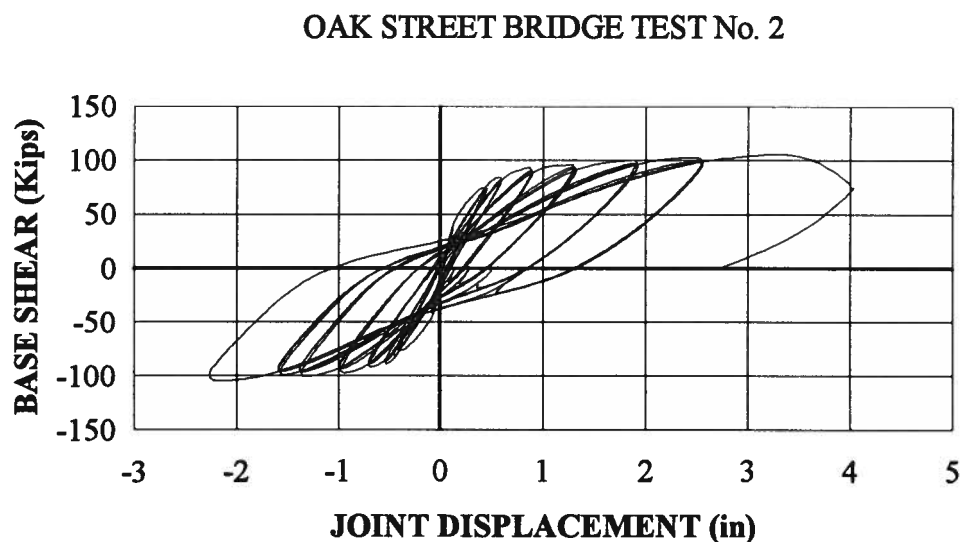


Fig 6.15 Hysteresis loop of bent test 2 (OSB2)

The cap beam of both the Joint specimen OJ1 and the Bent specimen OSB1 failed in shear (Fig.6.16 and 6.17). The major shear crack of OSB1 starts at the top of the cap beam exactly 5.0 ft away from the center line of the column. This crack propagates towards the column at angle of around 45 degrees. In the specimen OJ1, as the two bearing positions in the cap beam are 2'2" shorter than the full bent, the major shear crack originated closer to the column (4.0 ft from the center line of the column) and it extended at a much steeper angle (50 degrees) to the longitudinal axis of the cap beam (Fig. 6.18). The specimen OJ1 cap beam carried a maximum shear force of 49.7 kips at yield. This compares with the 53.6 kip shear force carried by the cap beam of specimen OSB1 (Appendix B Figs. B5 and B6).

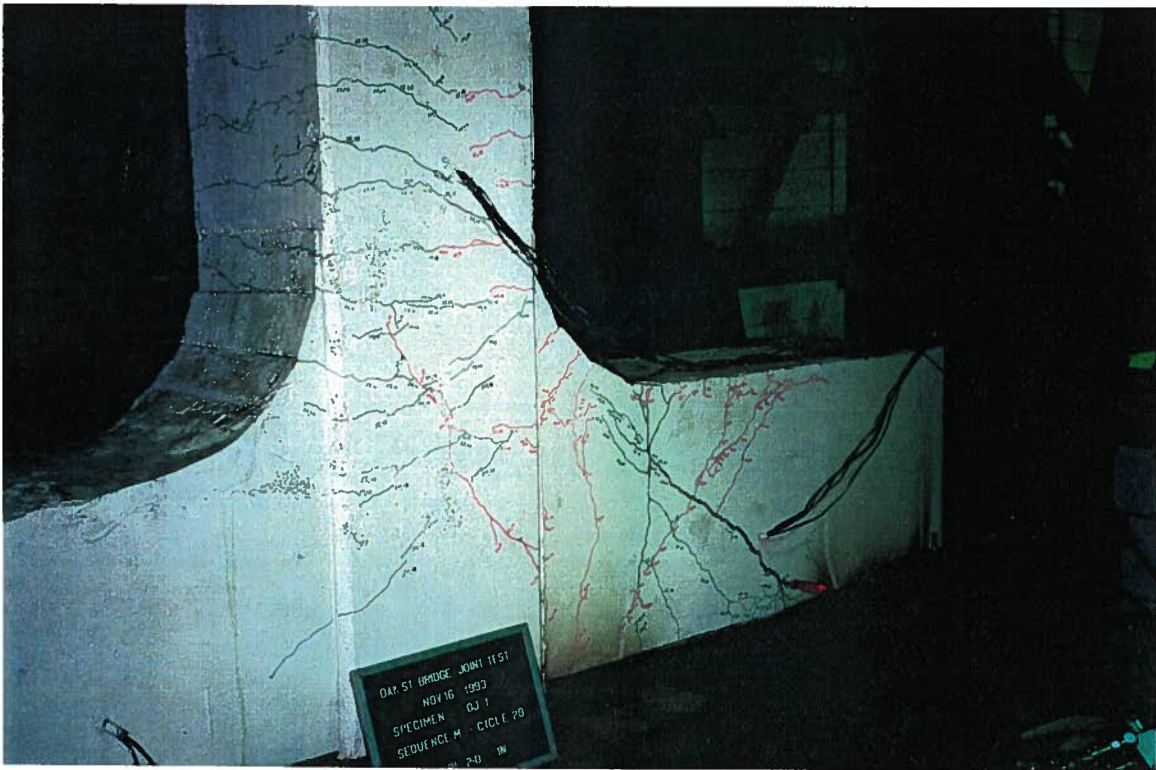


Fig.6.16 Cap beam cracking specimen OJ1



Fig. 6.17 Cap beam cracking Specimen OSB1

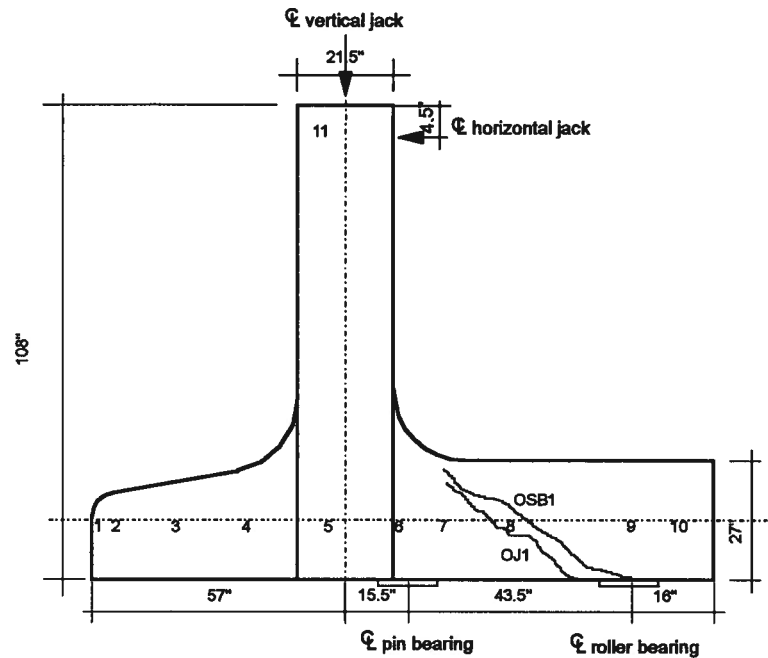


Fig. 6.18 Crack pattern of OJ1 and OSB1

In joint specimen OJ2 and bent specimen OSB2, the crack pattern and spacing of cracks in the columns are very similar to each other (Fig.6.19 and 6.20). Initially the column flexural cracks started closer to the joint and extended down to the middle of the column in the subsequent sequences. It is difficult to compare crack patterns at different sequences for the OJ2 and OSB2 specimens as the load displacement relationships were different. There were very few cracks in the cap beams of specimen OJ2 and OSB2 as compared to the Specimens OJ1 and OSB1. The shear force carried by the cap beam and the column of specimen OJ2 were 67.4 kips and 50.5 kips respectively. These values are comparable with the shear carried by the cap beam and the column of OSB2 80.2 kips and 56.4 kips respectively (Appendix B Figs. B13 and B14).

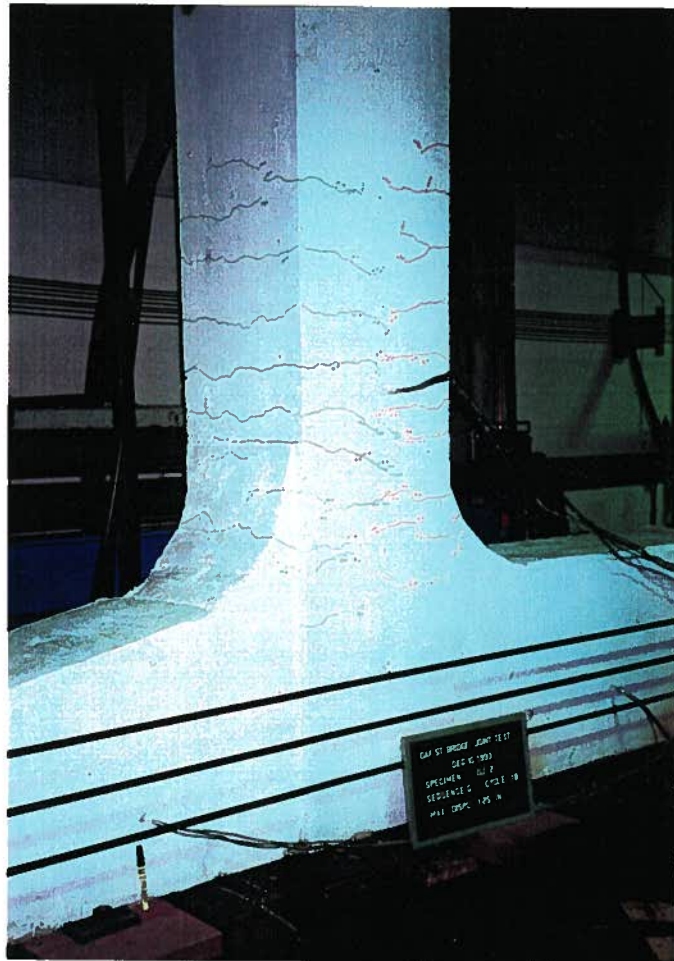


Fig. 6.19 Column cracking specimen OJ2

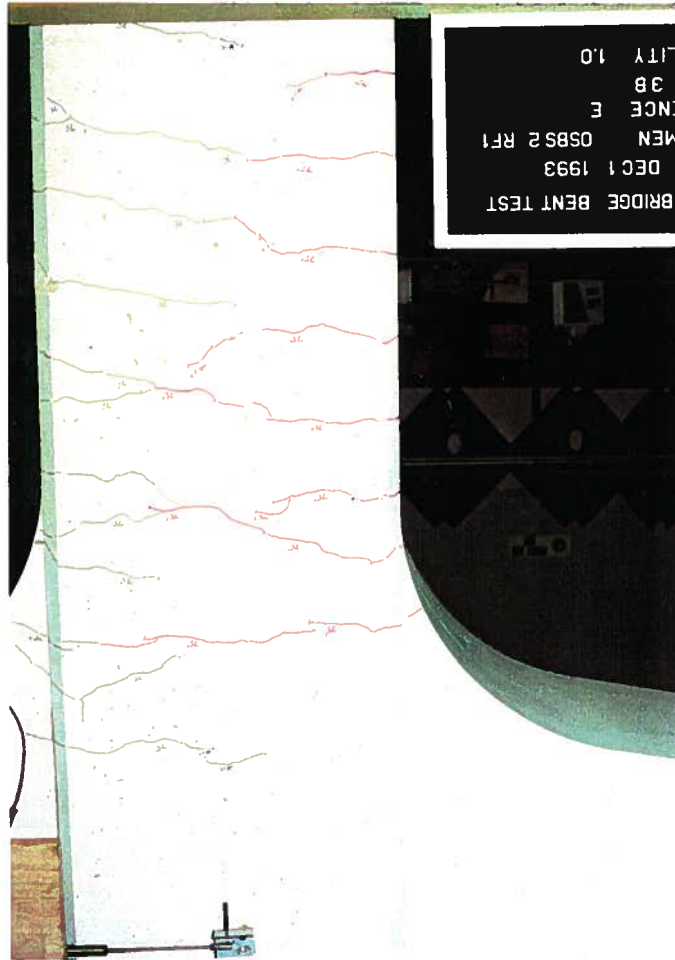


Fig. 6.20 Column cracking specimen OSB2.

## CHAPTER 7

### SUMMARY AND CONCLUSIONS

The two primary objectives of this project were to construct a test frame to test concrete components and to test two large scale specimens. Using the test frame, different inplane load combinations can be applied on different size specimens and configurations. i.e. joints, beams and columns. The number and the type of the boundary conditions at the bottom of the specimen can be changed to suit the test requirements. As the test frame is self equilibrated, external reactions are not required to equilibrate the jack loads applied during testing of the specimen.

To find out the behaviour of Oak Street Bridge bent due to lateral slow reversed cyclic loading, two half bent sections (as built and retrofitted) at 0.45 scale were tested. Both specimens were built using the existing material properties of the bridge. The full bent test were carried out by others and reported elsewhere (Anderson et al., 1994).

Brittle shear failure was anticipated in the cap beam of the as built specimens, i.e. in the middle third of the cap beam gage 4 stirrups were spaced at 1'4". Therefore cap beam of the first specimen was tested for anticipated shear force due to dead and lateral loading. Because of limitations in the equipment, particularly the inability to impose vertical load simulating dead load on the cantilever of the bent, a load system was organized that provided the required shear in the cap beam at section x-x, but did not fully duplicate the loading situation at the other sections. The cap beam of this specimen failed in shear as expected. The measured lateral load vs displacement hysteresis loops (Fig.6.1) showed

very significant strength degradation and pinching as expected. This particular mode of failure is associated with large deterioration of strength and stiffness which leads to sudden failure of the structure. The final failure mode of specimen OJ1 and OSB1 (MOTH full bent test) were similar (shear crack starting at the top of the cap beam and propagating towards the column). The specimen OJ1 cap beam carried a shear force of 49.7 kips at yield and the magnitude of the shear force carried by the specimen OSB1 at yield was 53.6 kips (Appendix B Figs. B5 and B6).

The cap beam of the second specimen was retrofitted by post-tensioning it with Dywidag bars. In the second specimen the loading pattern closely duplicated that of the full bent test for both the column and the cap beam. Post-tensioned cap beam of specimen OJ2 carried 35% higher shear force than that of OJ1 without any significant cracking in the cap beam (there is a small increase in shear capacity due to the increase of compressive strength of concrete of the second specimen from 26 MPa to 33 MPa). This increase in shear capacity of the cap beam indicates that the post-tensioning is an effective method of improving the shear capacity of the cap beam. This was verified by both full and half bent tests. The strains in the cap beam top and bottom bars of the post-tensioned specimen (OJ2) are very low due to the high compressive force in the cap beam compared to the as built specimen (OJ1). The last cycle (4" pushing) shows considerable stiffness degradation. As the stroke of the lateral loading jack was not sufficient, the specimens could not be loaded up to complete collapse.

Propagation of flexural cracking in the column of specimen OJ2 and OSB2 were similar. The large displacements of the column of the OJ2 specimen compared to the OSB2 specimen will result in a higher moment in the column due to the P- $\Delta$  effect of the

column axial load. The ultimate strengths (base shear) of specimen OJ2 and OSB2 were comparable, i.e. the applied maximum lateral load for OJ2, 50.5 kips was close to half the lateral load applied on the OSB2 which was 105.5 kips. The shear force carried by the cap beam and the column of the specimen OJ2 were 67.4 kips and 50.5 kips respectively. These values are comparable with the shear carried by the cap beam and the column of OSB2 which were 80.2 kips and 56.4 kips respectively (Appendix B Figs. B13 and B14).

There were large displacements of the OJ specimens compared to the OSB specimens. The main reason for this large displacements were the uplift at the roller bearing and the unexpected sliding at the pin bearing. The uplift could have been reduced by either tightening the bolts at the roller bearing or using a tie down at the roller bearing. The sliding at the bolts of the pin bearing could have been avoided by using a cylindrical roller as the pin bearing. It is also important to develop a more extensive displacement measurement system so that the displacements at the column tip of the half bent specimens can be related to the displacements at the joint of the full bent structure.

Although the stirrups and tie strain gauge values seems to be unreliable, most of the strain gauges in the main bars of the column and the cap beam of the two specimens showed reasonable strains.

This first series of tests on the test frame has demonstrated the ability to closely replicate tests on larger specimens, however there were a number of problem areas that could be improved in the future.

It is recommended that additional load capabilities be added. In the case of replicating tests such as the full bent tests, additional jacks could apply the equivalent dead load on the cantilever. The remaining limitation on the force system would be the lack of ability to impose flexure at the centerline of symmetry of the full bent. This is a dead load effect that becomes less important as the lateral load is increased.

A number of difficulties occurred due to the simplified bearing design. In a future test, it is recommended that further attention be given to the details of the bearings to eliminate even small vertical motions, which lead to overall rotation of the specimen. In addition, the bearing dimensions affect local conditions in the disturbed region. Since shear is of major importance, bearing details are also important.

The behaviour of the specimen could be monitored better if more extensive displacement measurements were made. It is recommended that these be devised to capture curvature and displacement throughout the specimen, and to establish the rigid body rotation so that actual displacements, relative to any reference system, can be readily determined.

## REFERENCES

Anderson, D., Sexsmith, R., and Seethaler, M., "Oak St. Bridge Two Column Bent Test", Report to the Ministry of Transportation and Highways, British Columbia, 1994.

Collins, M.P., and Mitchell, D., "Prestressed Concrete Structures ", Prentice Hall, 1991.

Hanson, N.W., Connor, H.W., "Seismic Resistance of Reinforced Concrete Beam-Column Joints " Journal of the Structural Division, ASCE, Vol. 93, No. ST5, Proc. Paper 5537, October 1967, pp 533-560.

Jirsa, J.O., Meinheit, D.F., and Woollen, J.W., "Factors Influencing the Shear Strength of Beam Column Joints " Proceedings of the U.S. National Conference on Earthquake Engineering, Ann Arbor, Mich., June 1975, pp 297-305.

Kawashima, K., and Koyama, T., "Effects of Cyclic Loading Hysteresis on Dynamic Behaviour of Reinforced Concrete Bridge Piers" Structural Eng./Earthquake Eng. Vol.5, No.2, 343s-350s, October 1988 Japan Society of Civil Eng.

Kennedy, D.W., Turkington, D.H., and Wilson, J.C., "Design for Earthquake Retrofit and Widening of the Vancouver Oak Street Bridge." Presented at CSCE Annual Conference Quebec City, May 1992.

Koyama, T., and Kawashima, K., "Effect of Number of Loading Cycles on Dynamic Characteristics of Reinforced Concrete Bridge Pier Columns" *Structural Eng./Earthquake Eng.* Vol 5. No.1,183s-191s, April 1988 Japan Society of Civil Engineers, Pg.205-213.

Leon, R.T., "Shear Strength and Hysteretic Behaviour of Interior Beam Column Joints", *ACI Structural Journal*, V.87, No.1, January-February 1990, Pg.3-11.

Meinheit, D.F., and Jirsa, J.O., "Shear Strength of Reinforced Concrete Beam Column Connections " November 1981, ASCE, Vol. 107, No. ST11.

Mitchell, D., Sexsmith, R., and Tinawi, R., "Seismic Retrofitting Techniques for Bridges - A State of The Art Report.", *CJCE*, Vol. 21, No. 2, April 1994.

Pantazopoulou, S., and Bonacci, J., "Consideration of Questions about Beam Column Joints" *ACI Structural Journal*, V.89, No. 1, January-February 1992, pg.27-36.

Park, R., and Paulay, T., "Behaviour of Reinforced Concrete External Beam-Column Joints Under Cyclic Loading " *Fifth World Conference on Earthquake Engineering, International Association for Earthquake Engineering, Rome, Italy, 1973, Paper No. 88, pp 772-781.*

Park, R., Rodriguez, M.E., and Dekker, D.R., "Assessment and Retrofit of a Reinforced Concrete Bridge Pier for Seismic Resistance", *Earthquake Spectra*, Vol. 9, NO. 4, 1993, Pg. 781-801.

Paulay, T., and Priestley, M.J.N., "Seismic Design of Reinforced Concrete and Masonry Buildings" John Wiley and Sons, Inc., 1991.

Pessiki, S.P., Conley, C., Bond, T., Gergely, P., and White, R.N., "Reinforced Concrete Frame Component Testing Facility Design, Construction, Instrumentation and Operation", National Center for Earthquake Engineering Research, SUNY, Buffalo, 1988.

Rogers, G.C., "A Seismotectonic Overview of the Pacific Northwest" EERI' 93 Annual Meeting, Seattle, Washington.

Seethaler, M., "Oak St. Bridge Bent Test Slow Cyclic Testing", M.A.Sc. Thesis, University of British Columbia, April, 1994.

CPCA, "Concrete Design Handbook", Canadian Portland Cement Association, Ottawa, 1985.

CISC, "Handbook of Steel Construction", Canadian Institute of Steel Construction, Ontario, 1984.

AASHTO, "Standard Specifications for Highway Bridges", Eighth Edition, 1961.

Canadian Standards Association, Design of Highway Bridges, CAN/CSA-S6-88, June 1988.

MOTH, "Seismic Rehabilitation of Bridges", Report by Ministry of Transportation and Highways, British Columbia, 1992.

## **APPENDIX A**

### **ANALYSIS AND DESIGN OF THE TEST FRAME**

In the initial analysis of the steel test frame a safety factor of 1.25 was used for the jack loads.

Analysis of the beam :

The top girder (AB) was analysed as simply supported. The two vertical jacks were assumed to be on either side of the center line of the girder.

Limits:

$$-1250 < P1 < 1250 \text{ kN.}$$

$$-1250 < P2 < 1250 \text{ kN.}$$

$$0 < a < 1.25 \text{ m}$$

$$0 < b < 1.25 \text{ m}$$

P1, P2 are vertical Jack Loads and a,b are horizontal distances by which those can be moved in each direction from the center line of the girder. In the analysis of the top girder two cases were considered. Those were when the vertical jacks acting in the same direction and when they were acting in the opposite direction.

Analysis of the column :

For the above locations and magnitudes of vertical jack loads assumed beam FG as fixed to find the end reactions and moments of the columns. (Fig. 2.2)

Columns were then designed for the maximum axial forces and moments found from the above analysis and for the horizontal jack force P3.

$$-1250 < P3 < 1250 \text{ kN.}$$

$$0.5 < C < 3.0 \text{ m}$$

Where P3 is the horizontal jack load and C the range of that jack

The truss members FD,DC,ED,BD were analysed as pinned and to carry the horizontal jack force of 1250 KN.

The floor beam was analysed for the following load cases.

1. When the vertical jack forces are in the same direction
2. When the vertical jack forces are in the opposite directions

For each case lateral loading jack direction and the position of each jack was changed to find the maximum reaction forces on the floor beam.

After analysing the structure for the above load cases initial sizing of members of the frame were done using the handbook of steel construction.(CAN3 - S16.1- M84 PART 1 )

Then using the computer program STAAD and with 32 load combinations confirmed the member loads and deflections are within the permissible values.

This frame is capable of supporting two 1000 kN. vertical jacks and one 1000 kN. horizontal jack. The maximum allowable forces and range of positions of the jacks are shown in Figure 2.1 The height of the horizontal girder ( W 610\*241 ) can be changed to suit the specimen size. For the above arrangement, the jacks are capable of exerting different combination of forces on required region of the specimen.

Maximum forces obtained using STAAD III / ISDS (SStructural Analysis And Design / Integrated Structural Design System)

Table A.1 Maximum frame member forces

MEMBER	B.M.(kNm)	SHEAR(kN.)	AXIAL(kN.)
GF	1200	1400	400
AG	1200	400	1400
FB	900	1000	1700
FC,ED,DB	0	0	1400
AC	800	1600	1000

In the girder to column joint design tried to reduce the moment transferred between members by assuming semi rigid connections. But the reduction in moment that can be achieved was negligible. Therefore reduced the vertical jack loads to the values shown in the Fig.2.1 And then the joints were analysed both as pinned and fixed and were design for the maximum forces obtained by those analysis.

## APPENDIX B

### FORCE RESULTANTS OF OJ1 AND OSB1

The Figs. B1 and B2 gives the maximum loading on OJ1 and OSB1. Figs. B3 to B8 are axial force , shear force and bending moment diagrams for maximum loading. Units are kip ft.

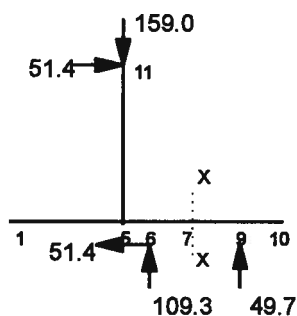


Fig. B.1 Maximum loading on OJ1  
(dimensions in Fig. 6.2)

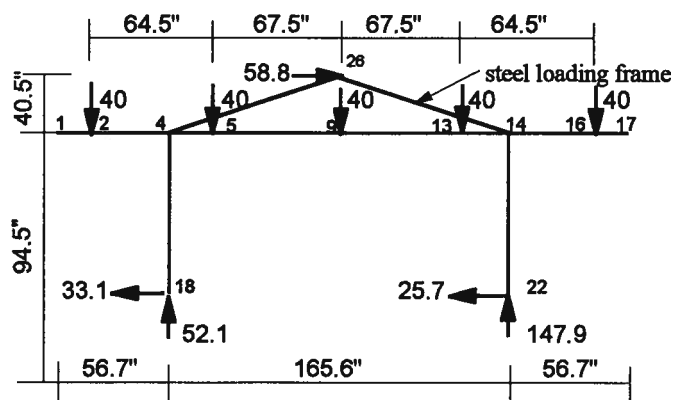


Fig. B.2 Maximum loading on OSB1

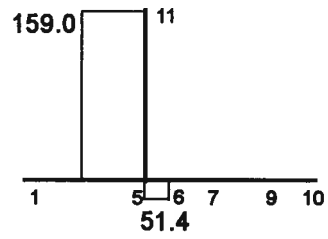


Fig. B.3 Axial force on OJ1

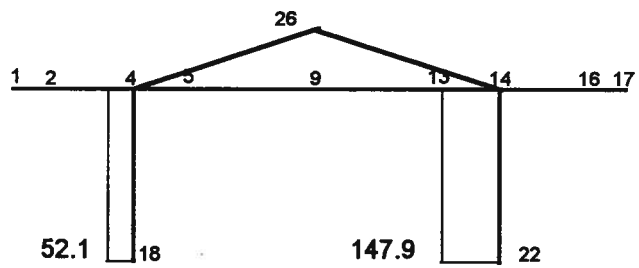


Fig. B.4 Axial force on OSB1

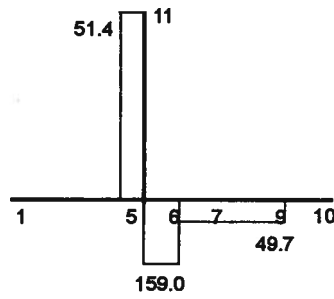


Fig. B. 5 Shear force on OJ1

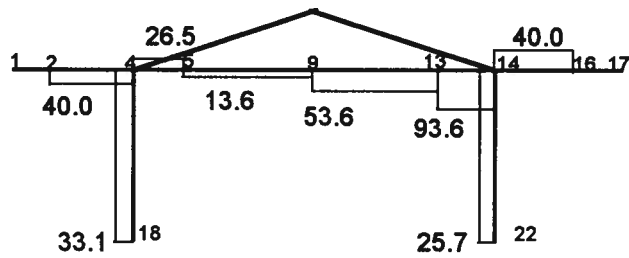


Fig. B.6 Shear force on OSB1

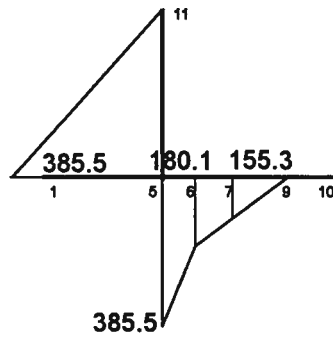


Fig. B.7 Bending moment on OJ1

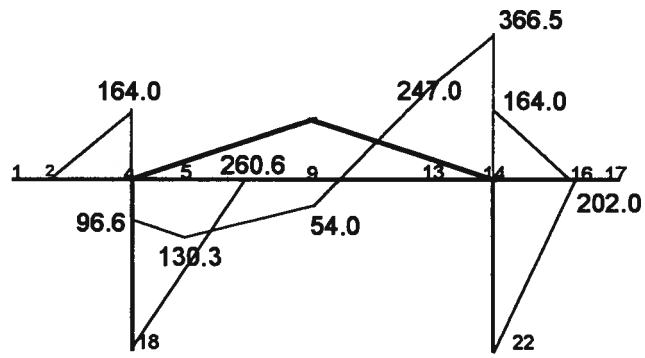


Fig. B.8 Bending moment on OSB1

## FORCE RESULTANTS OF OJ2 AND OSB2

The Figs. B.9 and B.10 gives the maximum loading on OJ1 and OSB1. Figs. B11 to B16 are the axial force, shear force and bending moment diagrams for maximum loading.

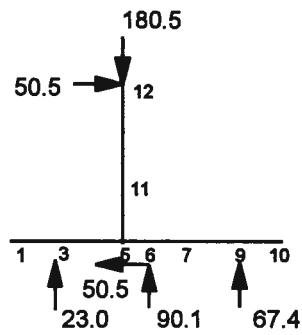


Fig. B.9 Maximum loading on OJ2  
(dimensions in Fig. 6.8)

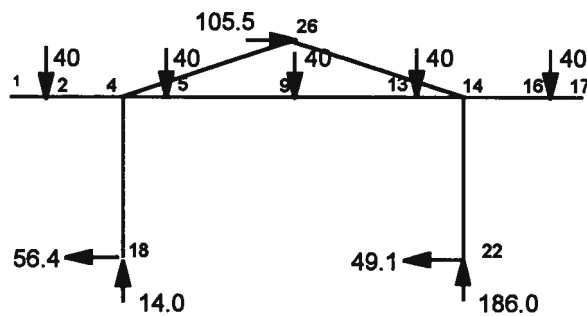


Fig. B.10 Maximum loading on OSB2

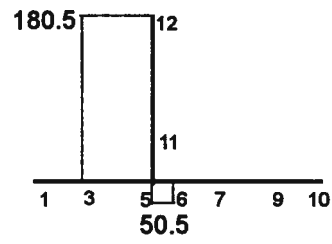


Fig. B.11 Axial force on OJ2

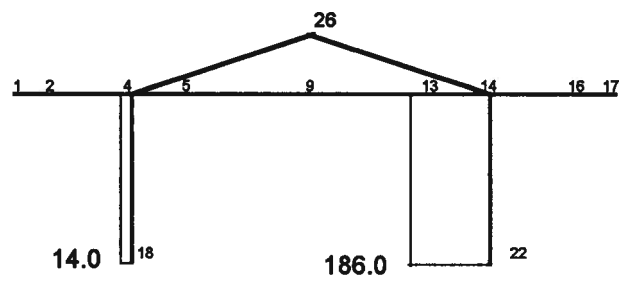


Fig. B.12 Axial force on OSB2

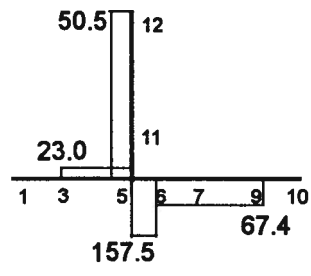


Fig. B.13 Shear force on OJ2

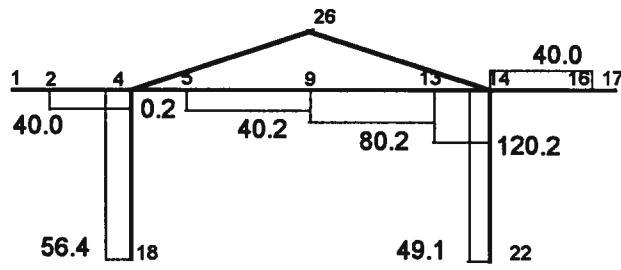


Fig. B.14 Shear force on OSB2

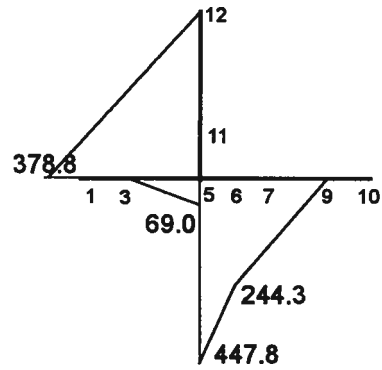


Fig. B.15 Bending moment on OJ2

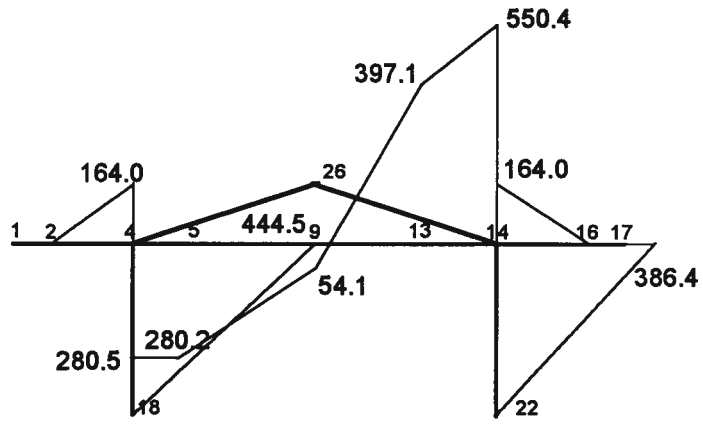


Fig. B.16 Bending moment on OSB2

## APPENDIX C

### JACK FORCES OF J2 AND J3

The Tables C.1 and C.2 gives the minimum and maximum J2 and J3 jack loads applied on the specimen OJ1 and OJ2 in each sequence.

Table C.1 Jack J2 min/max load

Sequence	min(kips)	max(kips)
A	97.2	105.5
B	73.5	116.8
C	72.5	119.4
D	73.7	125.9
E	69.4	136.8
F	63.1	141.6
G	54.0	146.4
H	42.7	158.1
I	31.8	159.0
J	17.0	150.0
K,L,O	27.5	155.0
P	13.3	137.7

Table C.2 Jacks J2 and J3 min/max load (J2 min. corresponds with J3 max.)

Sequence	J2 min(kips)	J2 max(kips)	J3 max(kips)	J3 min(kips)
A	97.6	110.0	44.9	41.4
B	90.0	113.6	47.2	40.2
C	79.1	131.7	50.4	34.9
D	67.8	147.2	53.7	30.3
E	59.5	157.8	56.2	27.2
F	46.0	170.2	60.1	23.6
G	37.5	179.0	62.6	23.3
H	33.9	182.1	63.7	23.0
I	32.6	180.5	64.1	23.0
J	32.6	180.2	64.1	20.8
K	29.5	198.2	64.9	15.3
L	30.5	191.3	64.7	17.3
M	25.1	149.6	66.3	29.6